Molecular Pharmacology Fast Forward. Published on December 7, 2020 as DOI: 10.1124/molpharm.120.000091
This article has not been copyedited and formatted. The final version may differ from this version.

$GABA_A$ RECEPTORS EXPRESSED IN OLIGODENDROCYTES CULTURED FROM THE NEONATAL RAT CONTAIN α3 AND γ1 SUBUNITS AND PRESENT DIFFERENTIAL FUNCTIONAL AND PHARMACOLOGICAL PROPERTIES

Rainald Pablo Ordaz, Edith Garay, Agenor Limon, Alberto Pérez-Samartín, María Victoria Sánchez-Gómez, Leticia Robles-Martínez, Abraham Cisneros-Mejorado, Carlos Matute, and Rogelio O. Arellano.

Instituto de Neurobiología, Laboratorio de Neurofisiología Celular, Universidad Nacional Autónoma de México, Juriquilla, Querétaro, México (R.P.O., E.G., L.R.-M., A.C.-M., R.O.A.).
Mitchell Center for Neurodegenerative Diseases, Department of Neurology, School of Medicine, University of Texas Medical Branch at Galveston, Galveston, USA (A.L.).
Achucarro Basque Center for Neuroscience, CIBERNED and Departamento de Neurociencias, Universidad del País Vasco (UPV/EHU), Leioa, Spain (A.P.-S., M.V.S.-G., C.M.).

Molecular Pharmacology Fast Forward. Published on December 7, 2020 as DOI: 10.1124/molpharm.120.000091
This article has not been copyedited and formatted. The final version may differ from this version.

Running title: **$GABA_AR$ molecular identity in oligodendrocytes**

Corresponding authors:
Dr. Rogelio O. Arellano
Instituto de Neurobiología, Universidad Nacional Autónoma de México.
Boulevard Juriquilla 3001, Juriquilla Querétaro, C.P. 76230, MÉXICO.
Phone: (5255) 56234062.
E-mail: arellano.ostoa@comunidad.unam.mx

Dr. Carlos Matute
Dpto. Neurociencias, Universidad del País Vasco, E-48940 Leioa, SPAIN.
Phone: 3494.6013244.
E-mail: carlos.matute@ehu.eus

Text pages: 56

Figures: 10

References: 63

Abstract: 241 words

Introduction: 742 words

Discussion: 1480 words

Abbreviations:

β-CCA, β-Carboline-3-carboxylic acid N-methylamide; β-CCB, N-butyl β-carboline-3-carboxylate; β-CCE, Ethyl 9H-pyrido[3,4-b]indole-3-carboxylate; β-CCt, tert-Butyl β-carboline-3-carboxylate; β-CHM, 3-(hydroxymethyl)-β-carboline; DIV, day(s) *in vitro*; DMCM, 4-Ethyl-6,7-dimethoxy-9H-pyrido[3,4-b]indole-3-carboxylic acid methyl ester; DZP, diazepam; FC, fractional contribution; FMZ, flumazenil; GFAP, glial fibrillary acidic protein; MBP, myelin basic protein; OL(s), oligodendrocyte(s); OPC(s), oligodendrocyte precursor cell(s); PDGFRα, platelet-derived growth factor receptor-α; siRNA, small interfering RNA.

Molecular Pharmacology Fast Forward. Published on December 7, 2020 as DOI: 10.1124/molpharm.120.000091
This article has not been copyedited and formatted. The final version may differ from this version.

ABSTRACT

Oligodendrocytes (OLs) express functional $GABA_A$ receptors ($GABA_ARs$) that are activated by GABA released at synaptic contacts with axons or by ambient GABA in extra-synaptic domains. In both instances, the receptors molecular identity has not been fully defined. Furthermore, data on their structural diversity in different brain regions, and information on age-dependent changes in their molecular composition, are scant. This lack of knowledge has delayed access to a better understanding of the role of GABAergic signaling between neurons and OLs. Here, we used functional, and pharmacological analyses, as well as gene and protein expression of $GABA_AR$ subunits, to explore the subunits combination that could explain the receptor functional profile expressed in OLs from the neonate rat. We found that $GABA_AR$ composed of α3β2γ1 subunits mimicked the characteristics of the endogenous receptor when expressed heterologously in *Xenopus laevis* oocytes. Either α3 or γ1 subunit silencing by siRNA transfection changed the GABA-response characteristics in oligodendrocyte precursor cells, indicating their participation in the endogenous receptor conformation. Thus, α3 subunit silencing shifted the mean EC_{50} for GABA from 75.1 to 46.6 μM, while γ1 silencing reduced the current amplitude response by 55%. We also observed that β-carbolines differentially enhance GABA responses in oligodendroglia as compared to those in neurons. These results contribute to defining the molecular and pharmacological properties of $GABA_ARs$ in OLs. Additionally, the identification of β-carbolines as selective enhancers of $GABA_ARs$ in OLs may help to study the role of GABAergic signaling during myelination.

Molecular Pharmacology Fast Forward. Published on December 7, 2020 as DOI: 10.1124/molpharm.120.000091
This article has not been copyedited and formatted. The final version may differ from this version.

SIGNIFICANCE STATEMENT:

GABAergic signaling through $GABA_A$ receptors ($GABA_ARs$) expressed in the oligodendroglial lineage contributes to the myelination control. Determining the molecular identity and the pharmacology of these receptors is essential to define their specific roles in myelination. Using $GABA_AR$ subunits expression and silencing, we identified that the $GABA_AR$ subunits combination α3β2γ1 conforms the bulk of $GABA_ARs$ in oligodendrocytes from rat neonates. Furthermore, we found that these receptors have differential pharmacological properties that allow specific positive modulation by β-carbolines.

Molecular Pharmacology Fast Forward. Published on December 7, 2020 as DOI: 10.1124/molpharm.120.000091
This article has not been copyedited and formatted. The final version may differ from this version.

INTRODUCTION

Oligodendrocytes (OLs) and their progenitor cells (OPCs) are endowed with membrane receptors sensitive to γ-aminobutyric acid (GABA), a key neurotransmitter in the central nervous system, suggesting an important role in the communication between neurons and oligodendroglial cells. Correspondingly, specific GABAergic synaptic neuron-OPC contacts have been demonstrated in several brain regions (Lin and Bergles, 2004; Jabs *et al.*, 2005; Kukley *et al.*, 2007; Káradóttir *et al.*, 2008; Tanaka *et al.*, 2009; Orduz *et al.*, 2015; Zonouzi *et al.*, 2015). Volume transmission has also been proposed as an important element for axon-glial chemical communication (Vélez-Fort *et al.*, 2010; Wake *et al.*, 2015). The main electrical response in OLs to GABA corresponds to the activation of a pentameric receptor-channel type A ($GABA_AR$), allowing the efflux of Cl^- ions, causing membrane depolarization and the subsequent opening of voltage-dependent Ca^{2+} channels (Gilbert and Kettenmann, 1984; Hoppe and Kettenmann, 1989; Kirchhoff and Kettenmann, 1992). This GABA response in OLs ultimately increases the intracellular Ca^{2+} concentration, which is involved in numerous phenomena, including the myelination process (Cesetti *et al.*, 2012; Cheli *et al.*, 2015, 2016; Wake *et al.*, 2015; Pitman and Young, 2016; Baraban *et al.*, 2018; Krasnow *et al.*, 2018). GABA sensitivity seems to be regulated throughout the course of OL maturation, with the lowest sensitivity observed in myelinating OLs in adulthood. Thus, the GABA response is maximal during postnatal development, a stage in which the premyelinating OLs contact with axons and initiate the myelinating program. It has been shown that GABA sensitivity is regulated by contact between the OLs and the axon through a mechanism that involves the regulation of protein subunit synthesis (Arellano *et al.*, 2016). Importantly,

Molecular Pharmacology Fast Forward. Published on December 7, 2020 as DOI: 10.1124/molpharm.120.000091
This article has not been copyedited and formatted. The final version may differ from this version.

$GABA_AR$s expressed in perinatal OLs and OPCs present distinctive characteristics that compared to those displayed in neurons and astrocytes (von Blankenfeld *et al.*, 1991; Bronstein *et al.*, 1998; Williamson *et al.*, 1998; Arellano *et al.*, 2016). Whether or not the $GABA_AR$ expressed during postnatal development has a similar molecular composition to the $GABA_AR$ expressed in OPCs at different ages or brain areas (especially in gray matter versus white matter) remains unknown, given that the observed characteristics and molecular identity indicate diversity in composition (see e.g., Vélez-Fort et al., 2012; Passlick et al., 2013; Balia et al., 2015).

It is fundamental to determine the $GABA_AR$ identity expressed in OLs during development, as well as its specific pharmacology, since GABAergic signaling is a prospect target for therapeutic strategies against demyelinating illness (e.g., Zonouzi et al., 2015; Shaw et al., 2018, 2019; Cisneros-Mejorado et al., 2019; Serrano-Regal et al., 2019). We proposed that the main receptor type in OLs and OPCs, from the optic nerve of P12 rats and forebrain of newborn rats, respectively, is comprised by a combination of the α3, β2 or β3, and γ1 or γ3 subunits (Arellano *et al.*, 2016). This is based on the functional and pharmacological profile of the GABA response in OLs and supported by information presented by distinct groups about the expression of $GABA_AR$ subunits in the oligodendroglial lineage. Accordingly, the most abundant mRNA expressed for α subunits is for α3 and α2 subunits, while γ2 and β1 subunit mRNA expression is absent or low in OPC preparations (Cahoy *et al.*, 2008; Larson *et al.*, 2016).

A characteristic that distinguishes the oligodendroglial receptor, with respect to neuronal $GABA_AR$s, is a positive modulatory effect of β-carbolines such as N-butyl-β-carboline-3-carboxylate (β-CCB; Arellano et al., 2016; Cisneros-Mejorado et al., 2019).

Molecular Pharmacology Fast Forward. Published on December 7, 2020 as DOI: 10.1124/molpharm.120.000091
This article has not been copyedited and formatted. The final version may differ from this version.

In this exploratory work, oligodendroglial $GABA_AR$ subunits were cloned and heterologously expressed in accordance with the studies cited above and on the analyses of publicly available RNA expression datasets in OPCs. Then, functional, and pharmacological analyses of six possible $GABA_AR$ combinations were performed. Their characteristics were compared with those displayed by the endogenous oligodendroglial $GABA_AR$. Priority was given to analyzing the possible binding site for β-CCB. Data showed that α3β2γ1 $GABA_AR$ closely mimicked the characteristics expressed by the endogenous receptor in OLs, including positive modulation by β-CCB that did not involve its binding to classic sites for benzodiazepines (BZD). Moreover, knocking down the expression of either α3 or γ1 subunits using the siRNA technique *in vitro* produced changes in the endogenous oligodendroglial GABA response, thus indicating that these subunits are involved in the receptor conformation. Finally, the effect of different β-carbolines, tested on both GABA responses from neurons and OLs, showed that many β-carbolines had a differential effect between these cell types, suggesting that they could be used to specifically enhance the $GABA_AR$ response expressed in OLs.

Molecular Pharmacology Fast Forward. Published on December 7, 2020 as DOI: 10.1124/molpharm.120.000091
This article has not been copyedited and formatted. The final version may differ from this version.

MATERIALS AND METHODS

Animal handling

All experiments were performed by trained personnel and conducted in accordance with the *Guide for the Care and Use of Laboratory Animals* by the National Institute of Health (USA). The animal protocols were approved by the Ethics Committees of the Instituto de Neurobiología at the Universidad Nacional Autónoma de México (UNAM) and the University of Basque Country (UPV/EHU). All possible efforts were made to comply with 3R standards and minimize animal suffering and the number of animals used.

RNA-Seq databases

Three datasets, derived from public domain resources as described below, were used for transcriptomic analysis (Figure 1A-B). Bulk RNA from mouse brain OPCs expressing platelet-derived growth factor receptor alpha (PDGFRα^{+}), a marker of OL progenitors (http://www.brainrnaseq.org; Zhang et al., 2014) were provided by Steven Sloan, who can be reached via the same website. Single cell datasets from three different regions in adult mice (P21-P90) were downloaded from the Gene Expression Omnibus (GSE75330; Marques et al., 2016) and the Allen Institute website (https://celltypes.brain-map.org/rnaseq; Tasic et al., 2016). From the first dataset, a total of 81 nuclei from cortex (S1), inferred as OPCs based on the cluster analysis reported previously, and 125 nuclei from the corpus callosum, were used. From the last dataset, a single cell analysis of the visual cortex (V1) in adult mice (P53-P59), thus normalized RNA-Seq from 30 NeuN^{-} nuclei, grouped in the OPC-PDGFRα^{+} cluster, were used in the analysis.

Molecular Pharmacology Fast Forward. Published on December 7, 2020 as DOI: 10.1124/molpharm.120.000091
This article has not been copyedited and formatted. The final version may differ from this version.

Detailed demographic characteristics, as well as technical white papers for data processing and quality control can be downloaded from the same site. Confirmatory analyses of enrichment of OPC markers and lack of neuronal markers were performed for all datasets. For data analysis, gene expression level in each dataset was transformed to fractional contribution (FC) to the total pool of mRNA available to produce $GABA_A$Rs (Sequeira *et al.*, 2019). Fractional contribution is defined as the percentage of expression level of each subunit gene over the sum of all 19 genes for $GABA_A$Rs subunits in each mouse/cell. The means of the FC for each gene in each single cell dataset (corpus callosum, S1 and V1 brain cortex) were averaged to build Figure 1A-B.

RT-PCR, cloning, and site-directed mutagenesis of $GABA_A$R subunits from OLs

To verify the expression of $GABA_A$R subunits, cDNA was synthetized from total RNA extracted from fresh isolated OLs derived from optic nerves of P12 rats (see below) and used in PCR assays. PCR products were amplified with the primers α3, forward: 5′-ACC ACA CAA ATG TGG CAC TTC-3′, reverse: 5′-AGT CAC TGC ATC TCC AAG CC-3′; β2, forward: 5′-ATG TGG AGA GTC CGG AAA AG-3′, reverse: 5′-TTT CAG TTG GGA GGC ACG TC -3′; β3, forward: 5′-CAC CCT GAT GGA ACA GTG CT-3′, reverse: 5′-ATG AGA GGA TTG TGA TCA TGA TTG-3′; γ1, forward: 5′-TAG GCG TGA GAC CCA CAG TA-3′, reverse: 5′-GCG ATT GGG CGT TGT TAT CC-3′; γ3, forward: 5′-ACC ATC AAT GCA GAG TGC CA-3′, and reverse: 5′-GCT GAG TGT GGT CAT GGT TA-3′. GAPDH amplification was used as a control with the oligonucleotide GAPDH, forward, 5′-TCC CTC AAG ATT GTC AGC AA-3′, and reverse, 5′-AGA TCC ACA ACG GAT ACA TT-3′. The PCR conditions were: an initial denaturation at 98°C for 30 s followed by 35 cycles at 98°C for 10 s, 55-60°C for 20 s, 72°C for 1 min, and finally 72°C for 5 min using

Molecular Pharmacology Fast Forward. Published on December 7, 2020 as DOI: 10.1124/molpharm.120.000091
This article has not been copyedited and formatted. The final version may differ from this version.

Phusion DNA Polymerase (Thermo Fisher Scientific; Waltham, MA, USA). The complete coding sequences for α3, β2, β3, γ1, γ2 and γ3 subunits were amplified using the primers: α3, forward: 5'-ATG ATA ACC ACA CAA ATG TGG C-3', reverse: 5'-CTA CTG TTT GCG GAT CAT G-3'; β2, forward: 5'-ATG TGG AGA GTC CGG AAA-3', reverse: 5'-TTA GTT CAC ATA GTA AAG CCA AT-3'; β3, forward: 5'-ATG TGG GGC TTT GCG GGA-3', reverse: 5'-TCA GTT AAC ATA GTA CAG CCA GT-3'; γ1, forward: 5'-ATG GGT TCT GGG AAA GTC-3', reverse: 5'-TTA TAA GTA TAG ATA TCC AAC CCA-3'; γ2, forward: 5'-ATG GCT GCA AAG CTG CTG-3', and reverse: 5'-TTA AAG ATA TAG GTA TCC AAC CC-3'; γ3, forward: 5'-ATG GCT GCA AAG CTG CTG-3', and reverse: 5'-TTA AAG ATA TAG GTA TCC AAC CC-3'. The PCR conditions were an initial denaturation at 98°C for 30 s followed by 35 cycles at 98°C for 10 s, 55-60°C for 20 s, 72°C for 1:10 min, and finally 72°C for 5 min. Each fragment obtained was cloned into pXENEX1 vector at the Ncol, BamHI and NotI sites (e.g., Pérez-Samartín et al., 2017). These plasmids were used as templates to make the site-directed mutagenesis of $GABA_AR$ subunits using the following primers: α3(H126R), forward: 5'-GGA CTC CAG ATA CCT TCT TCA GAA ACG G-3', reverse: 5'-GTG AGC CAC TGA TTT TTT ACC GTT TCT GAA G-3'; α3(S294I), forward: 5'-GTT CTC ACC ATG ACC ACC TTG ATC ATC AG-3', reverse: 5'-GGT AAA GAG TTT CTG GCA CTG ATG ATC AAG G-3'; β2(N264I), forward: 5'-CCT GAC GAT GAC CAC AAT CAT CAC CC-3', reverse: 5'-GAG TCT CCC GGA GAT GGG TGA TGA TT-3'; γ1(S282I), forward: 5'-CGG TTT TGA CTA TGA CAA CCC TCA TCA CA-3', reverse: 5'-GAA ACC TTA GGT AAA GAT TTT CTA GCG ATT GTG ATG AG-3', and the Pfu polymerase (Thermo Fisher Scientific; Waltham, MA, USA). Plasmids were linearized with the Hind III enzyme and used as templates for *in vitro* synthesis using the T7 mMESSAGE mMACHINE kit following the

Molecular Pharmacology Fast Forward. Published on December 7, 2020 as DOI: 10.1124/molpharm.120.000091
This article has not been copyedited and formatted. The final version may differ from this version.

standard protocol (Ambion, Invitrogen; Grand Island, NY, USA). cRNAs were used for heterologous expression in *Xenopus laevis* oocytes.

Heterologous functional expression of $GABA_AR$ subunits in *Xenopus* oocytes

Ovarian follicles of *Xenopus laevis* were dissected by surgery as described previously (Arellano and Miledi, 1993). Briefly, female *Xenopus laevis* frogs were obtained from Xenopus I (Ann Arbor, MI, USA). The ovarian lobules were surgically removed under sterile conditions from anesthetized frogs using 0.1% aminobenzoic acid ethyl ester (Sigma-Aldrich Co.; St. Louis, MO, USA) and rendered hypothermic. After surgery, frogs were sutured and allowed to recover from anesthesia. Frogs were maintained for 3 to 7 days in individual tanks until healing was complete and then housed in larger groups. No further oocytes were taken from them for at least 2 months. The follicles in stage VI (Dumont, 1972) were dissected from the lobules and maintained in normal Barth's solution (containing in mM: 88 NaCl, 1 KCl, 2.4 $NaHCO_3$, 0.33 $Ca(NO_3)_2$, 0.41 $CaCl_2$, 0.82 $MgSO_4$, 5 HEPES, adjusted to pH 7.4, and supplemented with 70 µg/mL gentamicin). Healthy isolated follicles were then injected with 50 nL of solution containing a mix of 2 or 3 (i.e., α3β2, α3β3, α3β2γ1, α3β2γ3, α3β3γ1, α3β3γ3 and α3β2γ2; in proportion 1:1 or 1:1:1) of the cloned $GABA_AR$ subunit cRNA sequences (5 ng per follicle), or with 50 nL H_2O as a control, and cells were incubated at 18°C in normal Barth´s solution. Then, 24 h post-injection, follicles were treated with 0.5 mg/mL collagenase type 1 A (Sigma-Aldrich Co.; St. Louis, MO, USA) in normal Ringer's (NR) solution (containing in mM: 115 NaCl, 5 KCl, 1.8 $CaCl_2$, and 5 HEPES; pH 7.0) for 30 min at room temperature. Cells were then washed several times with NR, and the oocytes were defolliculated using fine forceps under a stereomicroscope. Oocytes were

Molecular Pharmacology Fast Forward. Published on December 7, 2020 as DOI: 10.1124/molpharm.120.000091
This article has not been copyedited and formatted. The final version may differ from this version.

incubated at 18°C in Barth´s solution and monitored for their response to GABA and other drugs 3 to 6 days after cRNA injection. The electrical recording was made using the two-electrode voltage-clamp technique (Arellano and Miledi, 1993). For this, borosilicate glass micropipettes (filled with 3 M KCl) with a resistance of 1-2 MΩ were used. Currents were monitored using an Axon GenClamp 500B (Molecular Devices, San José CA, USA) amplifier, and signals were digitized and stored for further analysis using an analog-to-digital converter (Axon DigiData 1200, Molecular Devices) and specialized software (pClamp v9, Molecular Devices). For electrical recordings, the oocytes were continuously superfused (10 mL/min) at room temperature with NR (unless otherwise stated), voltage-clamped at −60 mV and applied periodic voltage steps to −40 mV (1 s) every 40 s during the recording to monitor membrane conductance. All experimental groups were replicated using oocytes from at least 3 different frogs.

GABA and $GABA_AR$ allosteric modulators were applied through the superfusion solution to test their effects on oocytes expressing the different $GABA_AR$ subunit combinations. Dose-response curves were fitted to the equation:

$$I/I_{max} = [(A1 – A2)/1 + ([GABA] / EC_{50})^{nH}] + A2 ,$$

by the method of nonlinear least-squares fitting, where EC_{50} is the half-maximal effective concentration for GABA, nH is the slope factor (Hill coefficient), A1 and A2 are the initial and final normalized current (I) values, respectively, and [GABA] is the concentration of the neurotransmitter. For the inhibitory effect generated by Zn^{2+} administration was calculated the half-maximal inhibitory concentration (IC_{50}) fitting D-R curves for Zn^{2+} with the same equation and method.

Forebrain OPCs, optic nerve OLs, and neuronal cell culture

Molecular Pharmacology Fast Forward. Published on December 7, 2020 as DOI: 10.1124/molpharm.120.000091
This article has not been copyedited and formatted. The final version may differ from this version.

Primary mixed glial cultures were prepared from newborn (P0-P2, of either sex) Sprague-Dawley rats as previously described (Arellano *et al.*, 2016; Sánchez-Gómez *et al.*, 2018). Briefly, forebrains were removed from the skulls, and cortices were isolated and digested by incubation (15 min, 37°C) in Hank's balanced salt solution containing 2.5% trypsin and 0.4% DNAse. The cells were dissociated by passage through needles (21G and 23G), centrifuged, and resuspended in Iscove's modified Dulbecco's medium supplemented with 10% fetal bovine serum (FBS; Hyclone Thermo Fisher Scientific, Waltham MA, USA) and antibiotic/antimycotic solution (Sigma-Aldrich Co., St Louis MO, USA). Cells were seeded into poly-D-lysine-coated (10 µg/mL) 75 cm^2 flasks and maintained in culture at 37°C and 5% CO_2. After 10-15 days in culture, the flasks were shaken (400 rpm, 2 h, 37°C) to remove loosely adherent microglia. The remaining OPCs on top of the confluent monolayer of astrocytes were dislodged by shaking overnight at 400 rpm. The cell suspension was then filtered through a 10 µm nylon mesh and plated on bacterial grade Petri dishes for 2 h. The non-adherent OPCs that remained in suspension were recovered and plated again on bacterial grade Petri dishes for 1 h. The resulting enriched forebrain OPC cell suspension was centrifuged and resuspended in a chemically defined medium (OPC medium) consisting of Dulbecco's modified Eagle's medium supplemented with 100 µg/mL transferrin, 60 ng/mL progesterone, 40 ng/mL sodium selenite, 5 µg/mL insulin, 16 µg/mL putrescine, 100 µg/mL BSA. Cells were plated onto poly-D-lysine-coated 12-mm-diameter coverslips in 24-well culture dishes at a density of $5x10^3$ cells per well and cultured in the presence of the mitogenic factors PDGF-AA (5 ng/mL) and bFGF (5 ng/mL) to expand their number and prevent their differentiation (here called proliferative medium). The purity of oligodendroglial cultures was confirmed by immunostaining with the antibodies against the oligodendroglial

Molecular Pharmacology Fast Forward. Published on December 7, 2020 as DOI: 10.1124/molpharm.120.000091
This article has not been copyedited and formatted. The final version may differ from this version.

markers PDGFRα, Olig2, and NG2 that labeled more than 80% of cells, indicating that these cultures contained mostly OPCs at this stage.

In addition to cortical OPC purification, primary cultures of OLs derived from optic nerves of 12-day-old Sprague Dawley rats of either sex were obtained as described previously (Arellano *et al.*, 2016). Cells were seeded on 24-well plates bearing 12-mm-diameter coverslips coated with poly-D-lysine (10 µg/mL) at a density of 10^4 cells per well. Cells were maintained at 37°C and 5% CO_2 in the differentiation medium. After 1-2 days *in vitro*, at least 97% of the cells were positive for the O4 antigen.

Primary cultures of cortical neurons were established according to a modified procedure (Larm *et al.*, 1996). Briefly, cortical lobes of Wistar rat embryos (E18, of either sex) were isolated and digested in Hank's balanced salt solution (Gibco; Thermo Scientific, Waltham MA, USA) containing 0.25% trypsin and 0.4% DNAse. After, the tissues were dissociated with needles (21G, 23G, 25G) and centrifuged. The neurons were resuspended in B27 neurobasal medium (Gibco Thermo Scientific) supplemented with 10% FBS (Hyclone, Thermo Fisher Scientific) and seeded at 10^5 cells per well onto poly-L-ornithine-coated (30 µg/mL) 24-well plates bearing coverslips with a 12-mm diameter. The medium was replaced by serum-free B27-supplemented neurobasal medium (with antibiotic-antimycotic and 2 mM glutamine) 24 h later. Cultures were maintained at 37°C and 5% CO_2. Rats were provided by the vivarium facilities either at the Instituto de Neurobiología at the Universidad Nacional Autónoma de México (UNAM) or at the University of Basque Country (UPV/EHU).

Whole-Cell Patch-Clamp

Molecular Pharmacology Fast Forward. Published on December 7, 2020 as DOI: 10.1124/molpharm.120.000091
This article has not been copyedited and formatted. The final version may differ from this version.

For the recording of membrane currents, cells (OPCs 1-4 DIV, OLs 1 DIV, or neurons 12-14 DIV) plated on coverslips were transferred to a recording chamber attached to a conventional inverted microscope (Olympus IX71; Tokyo, JP). They were continuously superfused and maintained at room temperature (22-25°C). The standard external solution (Attali *et al.*, 1997; Pérez-Samartín *et al.*, 2017) contained (in mM): 140 NaCl, 5.4 KCl, 2 $CaCl_2$, 1 $MgCl_2$, 10 (4)-(2-Hydroxyethyl)piperazine-1-ethanesulfonic acid (HEPES), and it was adjusted to pH 7.3 with NaOH. Electrophysiological recording was performed using either a MultiClamp 700B or an Axopatch 200B amplifier (Molecular Devices; Sunnyvale, CA, USA) to establish the standard whole-cell configuration. Patch-clamp pipettes (3-5 MΩ) were filled with internal solution (Pérez-Samartín *et al.*, 2017) containing (in mM): 140 KCl, 2 $CaCl_2$, 2 $MgCl_2$, 10 HEPES, 11 EGTA, 2 Na-ATP, and 0.2 GTP, adjusted to pH 7.3 with KOH. Currents were recorded at a holding membrane potential of −80 mV, digitized with an analog-to-digital converter (DigiData 1440; Molecular Devices, Sunnyvale CA, USA) and visualized and analyzed with specialized software (pClamp v10; Molecular Devices). In most cases, peak GABA current responses generated at −80 mV by drug superfusion were used for the analysis. Agonists and other drugs were added to the external solution from stock solutions, when necessary (e.g., for β-carboline application). DMSO was no more than 0.1% in the final solution.

Immunocytochemistry

To characterize primary cultures of OPCs and OLs, cells were immunoassayed with antibodies against oligodendroglial cell-specific markers: mouse anti-O4 (10 µg/mL; Ref. MAB345, Millipore, Burlington, MA, USA); mouse anti-PDGFRα (C-9) (1:200; Ref. sc-

Molecular Pharmacology Fast Forward. Published on December 7, 2020 as DOI: 10.1124/molpharm.120.000091
This article has not been copyedited and formatted. The final version may differ from this version.

398206, Santa Cruz Biotechnology, Dallas, TX, USA); rabbit anti-NG2 (1:300; Ref. AB5320, Millipore); rabbit anti-Olig2 (1:500; Ref. AB9610, Millipore); to detect myelin expression, the mouse anti-MBP was used (1:1000; Ref. SMI-99, Covance, Princeton, NJ, USA); astrocytes were identified by mouse anti-GFAP(2E1) (1:200; Ref. sc-33673, Santa Cruz Biotechnology). For α2, α3, γ1 and γ2 subunit immunostaining, cells were treated with the corresponding antibody (anti-$GABA_A$α2 1:100, Ref. AGA002; anti-$GABA_A$α3 1:100, Ref. AGA003; and anti-$GABA_A$γ1 1:100, Ref. AGA016; anti-$GABA_A$γ2 1:100, Ref. AGA005; from Alomone Labs, Jerusalem, IL). In all cases, cells were fixed in 4% paraformaldehyde in PBS for 30 min at RT. The fixed cultures were permeabilized with 0.1% Tween-20, blocked with 5% goat serum in PBS for 30 min and incubated overnight at 4°C with the antibodies diluted in PBS containing 5% goat serum and 0.1% Tween-20. Then, cells were rinsed and incubated for 2 h at room temperature with 1:200 goat anti-mouse IgG (H+L) conjugated with fluorescein isothiocyanate (FITC) (Ref. 81-6511, Invitrogen, Grand Island NY, USA) or 1:200 goat anti-rabbit IgG (H+L) conjugated with Alexa Fluor 514 (Ref. A-31558, Thermo Fisher Scientific, Waltham MA, USA) according to the host species of the primary antibodies. After five washes with PBS, samples were stained with 4’,6-diamidino-2-phenylindole dihydrochloride (4 μg/mL DAPI, from Molecular Probes, Eugene OR, USA) to identify cell nuclei. In all cases, the absence of nonspecific interactions of secondary antibodies was corroborated by omitting the primary antibodies. Finally, the samples were mounted on VectaShield (Vector Laboratories, Burlingame CA, USA), and the preparations were visualized under an LSM510 laser scanning confocal microscope or under an Apotome optical sectioning fluorescence microscope (both from Zeiss, Oberkochen, DE).

Molecular Pharmacology Fast Forward. Published on December 7, 2020 as DOI: 10.1124/molpharm.120.000091
This article has not been copyedited and formatted. The final version may differ from this version.

$GABA_AR$ subunit silencing by siRNA transfection

To reduce the expression of either α3 or γ1 subunit in cultured OPCs, the interference technique using small interfering RNAs (siRNAs) was used. These siRNAs were commercially designed (Dharmacon Inc., Lafayette CO, USA) for α3 (siGENOME Rat Gabra3 (24947) siRNA-SMARTpool) and γ1 (siGENOME Rat Gabrg1 (140674) siRNA-SMARTpool) using the target sequences NM_017069.3 and NM_080586.1, respectively. OPCs were seeded at a density of 4×10^4 cells per well in 24-well plates and allowed to attach overnight. Then, 1 DIV cells were transfected with 270 ng per well of α3-siRNA or γ1-siRNA using Lipofectamine 3000 (Invitrogen, Grand Island, NY, USA) following the manufacturer's instructions. For the control group (Control), cells were transfected in the same condition with the ON-TARGETplus Non-targeting Pool (SO-2686908G, Dharmacon Inc.). After 48 to 72 h of transfection, siRNA-treated OPCs maintained in culture were used for immunocytochemistry using the methods described above or for electrophysiological monitoring. The arbitrary units of fluorescence (AUF) were estimated as optical density using ImageJ software (version 1.52i). Briefly, applying blind analysis the intensity of green was obtained from five regions of interest (ROI) in every OPC preparation. AUF was calculated by normalizing the intensity values from each ROI against the background intensity value from each preparation, applying the following relationship: (intensity of the background – mean intensity of green measured in the ROIs)/intensity of the background (Cisneros-Mejorado *et al.*, 2019). Then, for α3-siRNA and γ1-siRNA transfected OPCs and their corresponding control groups, the AUFs were normalized against the respective untreated groups. The GABA response elicited in transfected OPCs with either α3-siRNA or γ1-siRNA were compared with those of the corresponding control groups, OPCs were identified in the culture by their typical bipolar

Molecular Pharmacology Fast Forward. Published on December 7, 2020 as DOI: 10.1124/molpharm.120.000091
This article has not been copyedited and formatted. The final version may differ from this version.

morphology and their rectifying I/V relationship, as well as for the basic characteristics of the GABA response such as its low sensitivity to GABA, inhibition by Zn^{2+} and/or enhancement by β-CCB (see supplementary Figures S2-S3).

Substances

7-Chloro-1-methyl-5-phenyl-3H-1,4-benzodiazepin-2(1H)-one (Diazepam, DZP); 4-Ethyl-6,7-dimethoxy-9H-pyrido[3,4-b]indole-3-carboxylic acid methyl ester (DMCM); N-butyl-β-carboline-3-carboxylate (β-CCB); β-Carboline-3-carboxylic acid N-methylamide (β-CCA); Ethyl 9H-pyrido[3,4-b]indole-3-carboxylate (β-CCE); 3-(hydroxymethyl)-β-carboline (β-CHM); tert-Butyl β-carboline-3-carboxylate (β-CCt); N-Methyl-N-[3-[3-[2-thienylcarbonyl]pyrazolo[1,5-a]pyrimidin-7-yl]phenyl]acetamide (indiplon); 8-Fluoro-5,6-dihydro-5-methyl-6-oxo-4H-imidazo[1,5-a][1,4]benzodiazepine-3-carboxylic acid, ethyl ester (Flumazenil, FMZ); were all obtained from Tocris Bioscience (Bristol, UK). Salts, DMSO, GABA and ATP were from Sigma-Aldrich Co. (St. Louis, MO, USA).

Statistical analysis

All data were analyzed using p-CLAMP (v.10.6, Molecular Devices, Sunnyvale CA, USA), R (v.3.2.3) with RStudio (Free Software Foundation Inc., Boston MA, USA) and GraphPad Prism (v.6.00, La Jolla CA, USA). Results are presented as mean ± S.D., regularly, the sample size and the number of experiments were adjusted after initial data collection and the final figures are indicated in each Figure or the text. The statistical significance of differences between two datasets was tested with an unpaired two-tailed Student's t-test. For multiple comparisons, a one-way ANOVA (Tukey's *post hoc* test) was used. The study was exploratory in nature and did not test a pre-specified null

Molecular Pharmacology Fast Forward. Published on December 7, 2020 as DOI: 10.1124/molpharm.120.000091
This article has not been copyedited and formatted. The final version may differ from this version.

hypothesis. The outcomes of the statistical tests cannot be interpreted as hypothesis testing but only as descriptive, thus, the indicated *p* values are therefore descriptive.

Molecular Pharmacology Fast Forward. Published on December 7, 2020 as DOI: 10.1124/molpharm.120.000091
This article has not been copyedited and formatted. The final version may differ from this version.

RESULTS

Cloning and expression of $GABA_AR$ subunits in OLs

To explore probable stoichiometries of $GABA_ARs$ expressed in OPCs, we examined the expression of all 19 genes for $GABA_AR$ subunits in cells isolated by fluorescence-activated cell sorting (FACS), measured in bulk (Bulk RNA-Seq) or individually (scRNA-Seq), from the cortex and corpus callosum, and deposited in public repositories (Zhang *et al.*, 2014; Marques *et al.*, 2016; Tasic *et al.*, 2016). Only cells that were positive to $PDGFR\alpha^+$, or clustered within the $PDGFR\alpha^+$ category, were used for this analysis. The FC (Sequeira et al., 2019) of each subunit to the total pool of mRNAs available to conform $GABA_ARs$ was analyzed in each dataset; results are illustrated in Figures 1A and 1B. In bulk RNA-Seq, α3 was the main expressed subunit, followed by β3 and β2, while γ1 was the main γ subunit (Figure 1A). In single cell RNA-Seq (Figure 1B), a similar result was obtained. Although α subunits did not present a clear preponderance, α3 was barely the major subunit, while β2, β3 and γ1 were well represented in the datasets. In both cases, γ2, γ3, β1, δ, as well as α5 and α6 subunits, were expressed at low or below the limit of detection levels. These results, together with the analysis reported previously (Larson *et al.*, 2016), are in agreement with previous functional studies (Arellano *et al.*, 2016) suggesting that $GABA_ARs$ in OLs from neonate rats are comprised by a combination of α3/β2-β3/γ1-γ3 subunits. Based on this information, we amplified, cloned and sequenced the five subunits from fresh OLs isolated from the rat optic nerve (P12) (Figure 1C). The sequences obtained indicate that all subunits were identical to those expressed in other cell types including neurons. Thus, the α3 subunit in OL was identical to the sequence NP_058765.3 (Malherbe *et al.*, 1990). The β2 and

Molecular Pharmacology Fast Forward. Published on December 7, 2020 as DOI: 10.1124/molpharm.120.000091
This article has not been copyedited and formatted. The final version may differ from this version.

β3 sequences were identical to NP_037089.1 (Ymer *et al.*, 1989) and NP_058761.1 (Ymer *et al.*, 1989), respectively, while γ1 and γ3 corresponded to sequences NP_542153.1 (Ymer *et al.*, 1990) and NP_077346.3 (Knoflach *et al.*, 1991), respectively. Protein expression was confirmed by immunodetection in OPCs isolated from neonate forebrain for α3, α2, and γ1 subunits, but γ2 expression was not detected in the same preparations (Figure 1D), as expected, the staining pattern for the analyzed subunits was different in cortical neuronal cells maintained *in vitro* (supplementary Figure S1). The cRNA for each subunit was transcribed and injected into oocytes to express distinct receptor combinations as follows: α3β2, α3β3, α3β2γ1, α3β2γ3, α3β3γ1 and α3β3γ3. The functional characteristics of the receptors expressed were studied electrophysiologically to compare their behavior with that described for the endogenous $GABA_AR$ expressed in OL. First, dose-response (D-R) curves for GABA were built for each receptor within the concentration range of 100 nM to 1 mM (Figure 2). All the subunit combinations expressed functional receptors, and the EC_{50} values estimated from the best fit for each normalized data set were as follows: α3β2, 19 ± 4.18 μM; α3β3, 10 ± 2.26 μM; α3β2γ1, 53 ± 4 μM; α3β2γ3, 21 ± 3.81 μM; α3β3γ1, 58 ± 2.26 μM; and α3β3γ3, 16 ± 2.22 μM (Figure 2A). In all cases, the Hill coefficient (nH) was within the range of 0.82-1.33. Two main differences were observed: 1) the maximal current amplitude was obtained with the combination α3β2γ1 that reached an average peak current of 9.37 ± 5.97 μA (n = 19 oocytes), while combinations α3β2γ3 and α3β3γ1 had peak currents of 2.36 ± 0.88 μA (n = 13 oocytes) and 4.43 ± 2.07 μA (n = 9 oocytes), respectively (Figure 2B); and 2) the highest EC_{50} values were obtained for receptors containing the γ1 subunit. These values were statistically different ($p < 0.05$) to those observed in receptors without the γ subunit or with γ3 (Figure 2C).

Molecular Pharmacology Fast Forward. Published on December 7, 2020 as DOI: 10.1124/molpharm.120.000091
This article has not been copyedited and formatted. The final version may differ from this version.

Sensitivity to Zn^{2+}

It has consistently been shown that GABA responses in OLs are inhibited by Zn^{2+} (100 μM; Williamson et al., 1998; Passlick et al., 2013; Arellano et al., 2016). This observation suggests the absence of the γ2 subunit, as it confers a relative insensitivity to the cation (Hosie *et al.*, 2003; Trudell *et al.*, 2008; Karim *et al.*, 2013), whereas the absence of any γ subunit renders $GABA_A$Rs highly sensitive to Zn^{2+}. However, it is not known whether γ1 or γ3 confers insensitivity as well as γ2 does, especially in combination with the α3 subunit. To achieve this information, we evaluated the effect of Zn^{2+} on the response elicited by GABA in oocytes expressing each of the combinations studied. Zn^{2+} and GABA were co-applied at 100 μM both, because this protocol inhibits more than 80% of the GABA response in receptors without γ subunits but has a weak effect on receptors with the γ2 subunit (e.g., Hosie et al., 2003; Karim et al., 2013). Figure 3 illustrates that the effect of Zn^{2+} on the peak of GABA response depended on the subunit combination expressed. Receptors without a γ subunit had the highest sensitivity to Zn^{2+} (67% to 85% of inhibition), receptors with γ3 presented lower sensitivity (20% to 32% of inhibition) and receptors with γ1 presented medium sensitivity to Zn^{2+} (within an inhibition range of 40% to 50%). For comparison purposes, the current response of the receptor α3β2 containing the γ2 subunit was inhibited around 10% in similar experiments. Thus, accordingly with several other studies where the participation of γ subunits greatly reduced the sensitivity to Zn^{2+}, this effect depended on the γ subunit type co-expressed in receptors containing α3β2 or α3β3 subunits. Among the different combinations tested in this condition, those that contained the γ1 subunit presented a

Molecular Pharmacology Fast Forward. Published on December 7, 2020 as DOI: 10.1124/molpharm.120.000091
This article has not been copyedited and formatted. The final version may differ from this version.

medium sensitivity to Zn^{2+}. A more detailed analysis was made to assess the potency of Zn^{2+} on receptors expressing this subunit.

The sensitivity to Zn^{2+} of the endogenous receptor in OPCs and OLs is about 10 μM testing the GABA response around its EC_{10}-EC_{30} (Arellano *et al.*, 2016). To compare the endogenous sensitivity with that displayed by heterologously expressed receptors, especially those containing the γ1 subunit, oocytes were injected with mRNA for α3β2γ1 or α3β3γ1 subunits, and these were compared with the receptor α3β2. Responses for each combination were generated applying 10 μM GABA alone (control condition) or together with distinct Zn^{2+} concentrations within the range of 0.1 to 1000 μM (traces in Figure 4A). Inhibition D-R curves were built for each receptor (Figure 4B), normalizing the peak current response in the presence of Zn^{2+} against the maximal control response without Zn^{2+}. The half-maximal inhibitory concentration (IC_{50}) values obtained were of 6.2 ± 2.68 μM, 25.7 ± 2.68 μM, and 69 ± 3.13 μM (5-7 oocytes for each case) for the receptors α3β2, α3β2γ1 and α3β3γ1, respectively; IC_{50} values were statistically different between all of them. This analysis shows that the receptor α3β2γ1 had an IC_{50} similar to that displayed by the endogenous receptor (Arellano *et al.*, 2016), while the α3β3γ1 receptor was less sensitive, as well as the α3β2 receptors in combination with either γ2 or γ3 subunit (Figure 4C), which had an IC_{50} for Zn^{2+} of 82.7 ± 2.69 μM and 75.5 ± 2.91 μM, respectively.

Effect of allosteric modulators on the α3β2γ1 $GABA_AR$

Molecular Pharmacology Fast Forward. Published on December 7, 2020 as DOI: 10.1124/molpharm.120.000091
This article has not been copyedited and formatted. The final version may differ from this version.

A battery of allosteric modulators was analyzed on the α3β2γ1 receptor expressed in *Xenopus* oocytes, considering that this combination presented closer parameters of sensitivity to GABA and Zn^{2+} to those exhibited by receptors endogenously expressed in OLs; this combination is also in accordance with the transcriptomic analysis reported. The positive modulators DZP, indiplon and β-CCB were analyzed by applying the respective EC_{10} for GABA, as a control response, and the same concentration of GABA in co-application with each drug. Each modulator was applied alone for 40 s prior to co-application with GABA (Figure 5A). Both DZP and β-CCB enhanced the response to GABA by 198.0 ± 37.2% (11 oocytes) and 236.4 ± 40% (11 oocytes), respectively, while indiplon had a weak or null effect on the response (110.5 ± 3.65%, 10 oocytes) (Figure 5B). In general, the effect of these modulators on the receptor α3β2γ1 were like those displayed by the endogenous $GABA_AR$ expressed in OLs. The interaction of β-carboline with α3β2γ1 was analyzed in greater detail (Figure 5C). The positive effect of β-CCB (30 μM) was not blocked by flumazenil (FMZ; 10 μM), a classic BZD site antagonist; in fact, application of FMZ together with β-CCB caused a greater response of the α3β2γ1 receptor, as illustrated in Figure 5C. Thus, the enhancement caused by β-CCB without FMZ was of 324.1 ± 74%, whereas in the presence of FMZ was of 446.9 ± 65% (17-20 oocytes in each case). This result suggested that the β-CCB binding site did not correspond to the classic BZD binding site, an observation that was supported by similar co-application experiments with β-CCB and GABA at α3β2γ3 and especially α3β2 receptors in which the β-carboline also caused an important increase of the response (Figure 5D).

To confirm this result, the specific binding sites of high and low affinity to BZD were mutated on the α3, β2, and/or γ1 subunits. Thus, the α3β2γ1 receptor sensitivity to DZP

Molecular Pharmacology Fast Forward. Published on December 7, 2020 as DOI: 10.1124/molpharm.120.000091
This article has not been copyedited and formatted. The final version may differ from this version.

was eliminated or strongly decreased similarly to the manner previously shown for the neuronal receptor (Benson *et al.*, 1998; Walters *et al.*, 2000; Middendorp *et al.*, 2015). The results of these experiments are illustrated in Figure 6. First, the H126R mutation in the α3 subunit eliminated the sensitivity to 1 μM DZP (Benson *et al.*, 1998). However, positive modulation caused by β-CCB (1 μM) on the response to GABA (10 μM) was not affected, being 144.8 ± 18% in the oocytes expressing the native receptor and 202.4 ± 17.4% in the mutated receptor α3(H126R)β2γ1 (5-6 oocytes from 2 frogs; Figure 6A). Also, mutations α3(S294I)β2(N264I)γ1(S282I) were made to eliminate one of the low-affinity BZD sites located in the transmembrane region (Walters *et al.*, 2000), and this receptor was expressed to explore its sensitivity to 60 μM DZP and 1 μM β-CCB. The results illustrated in Figure 6B indicate that the potentiation of the GABA (10 μM) response produced by co-application of 60 μM DZP was greatly reduced in the mutant receptor α3(S294I)β2(N264I)γ1(S282I) compared to the α3β2γ1 receptor response. The values were 281.1 ± 25% for the latter and 172.3 ± 10% for the mutant receptor, where persistent potentiation in this case was more likely due to DZP interaction on the high-affinity site. However, β-CCB application to the α3(S294I)β2(N264I)γ1(S282I) receptor maintained a positive modulatory effect and enhanced the response by 251.6 ± 10.5% versus the control native receptor that presented an increase of 160.1 ± 8% (10 oocytes). These data support the idea that β-CCB did not act on the classic BZD site of the $GABA_A$ α3β2γ1 receptor, but also did not act on the described transmembrane low-affinity site for BZD.

Effect of β-carbolines on the endogenous response to GABA in OLs and neurons

Molecular Pharmacology Fast Forward. Published on December 7, 2020 as DOI: 10.1124/molpharm.120.000091
This article has not been copyedited and formatted. The final version may differ from this version.

The effect of β-CCB acting on a different binding site to that of high-affinity for BZP on the α3β2γ1 receptor is similar to the effect observed for the endogenous oligodendroglial $GABA_AR$. Figure 7 illustrates that the endogenous response to 10 μM GABA in cultured OLs isolated from optic nerve was enhanced by β-CCB (10 μM), but not affected by FMZ (10 μM) (n = 7). These results suggest that β-CCB did not act through the interaction with the high-affinity site for BZP in the endogenous $GABA_AR$ in OLs. In contrast, FMZ did block the potentiation of the response to GABA mediated by DZP (10 μM) either in OLs (n = 7) or cortical neurons (n = 5) (Figure 7A). Nevertheless, in this case FMZ did not cause an extra-enhancement of the GABA response when tested in conjunction with β-CCB.

Also, it was observed that in the endogenous response, β-CCB enhancement was mainly due to an increase in the sensitivity to GABA, shown in Figure 7B, where D-R curves for GABA were built in both the absence and presence of β-CCB (10 μM). Thus, in the absence of the modulator, the EC_{50} was of 83.3 ± 8.6 μM (n = 5); whereas in the presence of β-CCB, the EC_{50} was of 18.5 ± 3.4 μM (n = 6), the EC_{50} differences were statistically significant (*$p<0.001$ for comparisons across the mean of $-\log EC_{50}$ values from each group, one-way ANOVA followed by a Tukey´s *post hoc* test). The last EC_{50} value was also similar to that observed in the presence of β-CCB for the α3β2γ1 receptor heterologously expressed.

A particularly important aspect of β-carboline action is the probable differential effect on the oligodendroglial receptor, compared with the effect on receptors expressed in neurons. In order to obtain more information about this effect, the potency for different β-carbolines on GABA responses in both OLs and cortical neurons maintained in culture

Molecular Pharmacology Fast Forward. Published on December 7, 2020 as DOI: 10.1124/molpharm.120.000091
This article has not been copyedited and formatted. The final version may differ from this version.

was explored. It has been shown that β-CCB distinguishes between the receptors expressed in these two cell types (Cisneros-Mejorado *et al.*, 2019). Here we confirmed this differential effect analyzing the effect of a battery of distinct β-carbolines on the endogenous GABA response of OLs and neurons. Figure 8 illustrates that the endogenous response to GABA in OLs or neurons (EC_{10} in each case) was monitored in the absence (control response) or presence of one of distinct β-carbolines. The normalized response with respect to the control is indicated as an average of the effect in the tested cells. The β-carboline (10 μM) positive modulatory effect on the response to GABA (10 μM) in OLs presented the following power sequence: β-CCB > β-CCA > β-CCE > β-CCt > β-CHM (Figure 8A), while DMCM inhibited the response. In contrast, most of the β-carbolines (same concentration) presented either a net inhibitory effect on the neuronal receptor activated by 3 μM GABA or did not have a clear effect on the amplitude of the response, as observed for β-CCB or β-CCE (Figure 8B). Thus, it appears that distinct β-carbolines presented a differential effect on the oligodendroglial $GABA_AR$. For β-CCB, this effect was not due to its interaction with the high-affinity binding site for BZP.

Specific silencing of endogenous α3 or γ1 $GABA_AR$ subunits in OLs

Since α3 and γ1 subunits appear to define important characteristics of the endogenous oligodendroglial receptor, we performed the following experiments to directly determine their participation in the receptor conformation. For this, transfections with specific siRNA were performed for each subunit in OPCs isolated from neonate forebrain. Before performing the GABA response analysis in the transfected cells, OPCs were monitored

Molecular Pharmacology Fast Forward. Published on December 7, 2020 as DOI: 10.1124/molpharm.120.000091
This article has not been copyedited and formatted. The final version may differ from this version.

for at least 4 days *in vitro* to evaluate essential characteristics such as marker expression (NG2, PDGFRα, MBP) and the electrophysiological and pharmacological GABA response profile. This was necessary because the maximal silencing effect of the respective protein had a 48-h temporality. The result of this analysis indicated that most (85 to 90%) cells maintained in culture from 2 DIV to 4 DIV in proliferating medium showed characteristics corresponding to OPCs expressing Olig2, NG2 and PDGFRα, but not GFAP or MBP, while at 4 DIV a significative percentage (21.6 ± 4.85%) of cells expressed O4 and presented a more complex morphology (supplementary Figure S2). Importantly, the $GABA_AR$ functional and pharmacological profile expressed did not change during the culture time from 2 DIV to 4 DIV. The I/V electrophysiological profile did not show statistically significant differences either (supplementary Figure S3), especially with regard to the typical rectifying behavior, due to the lack of Kir-type current activated at hyperpolarizing potentials (Pérez-Samartín et al., 2017). Thus, OPCs at 2 DIV were transfected with specific siRNA against either α3 (Figure 9) or γ1 (Figure 10) subunits, and the effect of this manipulation was compared with respect to cells that were transfected with a nonspecific siRNA (control), using the expression in untreated cells as reference. As illustrated in Figure 9A, α3-siRNA transfection strongly reduced (93.7 ± 2%) the expression of the respective subunit as evidenced by the corresponding immunodetection, while transfection with nonspecific siRNA did not cause a notable α3 subunit expression decrease. The current amplitude generated by 1 mM GABA showed no change between these cell groups (1795.4 ± 1393 pA in control cells vs. 1539.3 ± 653 pA in α3-siRNA treated cells), although the GABA response showed three important changes. First, α3-siRNA treated cells showed an increase in the GABA response

Molecular Pharmacology Fast Forward. Published on December 7, 2020 as DOI: 10.1124/molpharm.120.000091
This article has not been copyedited and formatted. The final version may differ from this version.

desensitization rate, as illustrated in Figure 9B. This figure shows that control cells displayed a response desensitization fitted to an exponential decay with a mean time constant of 2109.2 ± 1321 ms, while the transfected cells presented desensitization time constants with an average of 1190 ± 253 ms (15-25 cells in each group; from 4 distinct transfections). Second, D-R curves constructed for these two experimental groups (Figure 9C) showed that α3 subunit silencing caused an increase in the sensitivity of the expressed receptor and that the control EC_{50} of 75.1 ± 4.12 μM decreased to 46.6 ± 3.8 μM in α3-siRNA transfected cells (n = 10), a statistically significant difference. And third, α3-siRNA transfected cells also showed a decrease in sensitivity to β-CCB (10 μM) co-applied with GABA (10 μM), and generated a weaker increase of the GABA response to 156.4 ± 32.2 % (9 cells) compared with the control effect of 227.26 ± 62.2 % (10 cells) as illustrated in Figure 9D.

γ1 subunit silencing in OPCs also caused changes, and although γ1 protein expression was not reduced by γ1-siRNA transfection as strongly as that designed against α3, the effect reached a 71 ± 1.6% decrease at 4 DIV as evidenced by immunodetection (Figure 10A-B). However, the γ1 expression decrease was accompanied by an average amplitude diminution of GABA (1 mM) peak response compared to the respective control of 55.1 ± 1.5% (1795.4 ± 1393 pA vs. 805.6 ± 463 pA). In this case, the corresponding EC_{50}´s for both groups did not show a statistically significant difference (75.1 ± 4.12 μM for the control group vs. 88.9 ± 3.48 μM for γ1-siRNA transfected cells;

Molecular Pharmacology Fast Forward. Published on December 7, 2020 as DOI: 10.1124/molpharm.120.000091
This article has not been copyedited and formatted. The final version may differ from this version.

10-15 cells in each case, 4 different transfections) (Figure 10C). In similar manner to that showed for α3-siRNA transfected cells, the γ1-siRNA transfected cells were less sensitive to β-CCB, and in the presence of the β-carboline the GABA-response was barely enhanced to 113.2 ± 16.6% while the control group (same than control in Figure 9D) was increased to 227% (Figure 10D). These results showed that both subunits, α3 and γ1, seem to participate in the conformation of the endogenous receptor. They also suggested that the absence of α3 was compensated by another subunit, whereas γ1 subunit expression was essential to maintain the GABA response in OPCs as well as their sensitivity to β-CCB.

Molecular Pharmacology Fast Forward. Published on December 7, 2020 as DOI: 10.1124/molpharm.120.000091
This article has not been copyedited and formatted. The final version may differ from this version.

DISCUSSION

The molecular mechanisms responsible for the control of myelination are only partially known and their definition will help to identify new therapeutic targets for the treatment of various pathological conditions. GABA signaling participates in myelination (Zonouzi *et al.*, 2015; Arellano *et al.*, 2016; Balia *et al.*, 2017; Hamilton *et al.*, 2017; Kalanjati *et al.*, 2017; Shaw *et al.*, 2018; Cisneros-Mejorado *et al.*, 2019; Kalakh and Mouihate, 2019; Serrano-Regal *et al.*, 2019); however, its specific functional role and mechanisms involved are not completely understood. To progress in these issues, this study aimed to determine the molecular identity of the main $GABA_AR$ expressed in the oligodendroglial lineage, especially in OPCs and OLs from newborn rats (Arellano *et al.*, 2016). The results indicated that the receptor composition includes the α3 and γ1 subunits, while the most likely β subunit involved is β2. The identity proposed here, α3β2γ1, agrees with other studies proposing a composition α3/β2 or β3/γ1 or γ3 from a pharmacological and functional perspective (Arellano *et al.*, 2016), and with the transcriptomic analysis performed in $NG2^+$ cells (Larson *et al.*, 2016), where the mentioned subunits have a high expression level. The transcriptomic analysis presented here in $PDGFR\alpha^+$ cells confirmed the expression of the coding sequences for various subunits, where the α2 and α3 subunits, together with β2, β3, and γ1, were all well represented. This analysis also highlighted the low or null expression of γ2, γ3, and δ subunits. Thus, coincidentally, a similar group of subunits was suggested from all the transcriptomic analyzes described and the set of subunits proposed from the functional studies, regardless of the murine species, age, and brain region. This concordance supports the the relevant contribution of α3, β2 and γ1 subunits to $GABA_AR$ in cultured OLs from the

Molecular Pharmacology Fast Forward. Published on December 7, 2020 as DOI: 10.1124/molpharm.120.000091
This article has not been copyedited and formatted. The final version may differ from this version.

neonatal brain, but clearly does not exclude participation of other subunits for which solid evidence of their expression has been found in certain areas of the nervous system, and in different stages of development (Passlick et al., 2013; see also, Serrano-Regal *et al.*, 2020).

$GABA_AR$ subunits protein expression was confirmed by immunodetection in cultured OLs and OPCs from the forebrain, and transcripts of α3, β2, β3, γ1 and γ3 subunits were subsequently amplified from OLs isolated and purified from rat optic nerve; the corresponding genes were cloned, and cRNA synthesized *in vitro* was expressed into *Xenopus laevis* oocytes to analyze the functional characteristics of 6 possible receptors. Their characteristics were compared with those shown by the endogenous receptors reported previously (e.g., Arellano *et al.*, 2016) to determine which combination most closely reproduced the endogenous GABA response. Results studying GABA sensitivity showed that α3β2γ1 was the most efficient in terms of amplitude response, it remains unknown if this represents an intrinsic condition for preferential assemble. However, it is important to note that substitution of β2 by β3 results in an important decrease in the amplitude of the GABA responses.

$GABA_ARs$ with α3β2γ1 subunits have an EC_{50} of 53 μM. Substitution of β2 by β3 in this combination did not change GABA responses, whereas substitution of γ1 by γ3 caused a 3-fold increase in GABA-sensitivity. Hence, the EC_{50} value for the heterologously expressed α3β2γ1 is close to that of the endogenous receptor, as all reports so far indicate an EC_{50} for GABA between 70-100 μM (e.g., Arellano *et al.*, 2016).

On the other hand, Zn^{2+}-sensitivity is a key parameter for this comparison because high sensitivity is an indicator of γ subunit absence. It was demonstrated that compared with γ2 and γ3 subunits, γ1 confers moderate Zn^{2+}-sensitivity, furthermore, it was also clear

Molecular Pharmacology Fast Forward. Published on December 7, 2020 as DOI: 10.1124/molpharm.120.000091
This article has not been copyedited and formatted. The final version may differ from this version.

that β subunit substitution also affected this parameter. The receptors containing the γ1 subunit were studied further applying (10 μM) GABA and constructing D-R curves for Zn^{2+}. The α3β2γ1 conformation presented an IC_{50} of 25 μM, which was similar to the value observed in the endogenous receptor, while the substitution of β2 by β3 increased 3-fold this parameter. Therefore, the combination containing β2 is closer to the endogenous value. Additionally, by comparing the IC_{50} values for receptors containing the combination α3β2 with, or without a γ subunit, once again α3β2γ1 presented the closest IC_{50} value to that described for the endogenous receptor.

The combination α3β2γ1 also presented an endogenous-like sensitivity for allosteric modulators, such as DZP, indiplon, and the β-carboline β-CCB. The β-CCB effect is important because it distinguishes between receptors expressed either in OLs or neurons. Given that this drug has the potential for specifically promoting GABAergic signaling in OLs *in vivo* (Arellano *et al.*, 2016; Cisneros-Mejorado *et al.*, 2019), it was critical to explore in detail the action of β-CCB on the α3β2γ1 receptor. Results indicated that β-CCB effect did not require interaction with the classic BZP binding site, since it was not antagonized by FMZ. Instead, FMZ caused a greater enhancement, suggesting, as proposed before (Sieghart, 2015), that β-CCB had a dual effect in which the classic site promoted inhibition (i.e., the inverse agonist effect) and a second site caused the positive modulatory effect. Studies have suggested that this potentiation site for β-carbolines might include residues conforming the low-affinity binding site for DZP located in the second transmembrane domains of α, β, and γ subunits (Walters *et al.*, 2000). This is supported by results showing that the α3β2 receptor is still potentiated by β-CCB. Because subunit substitution might represent a more complex change in the final binding site configuration, we performed point mutations in α3β2γ1 to eliminate the

Molecular Pharmacology Fast Forward. Published on December 7, 2020 as DOI: 10.1124/molpharm.120.000091
This article has not been copyedited and formatted. The final version may differ from this version.

high and low affinity DZP binding sites. Mutations eliminated DZP sensitivity as described for γ2-containing receptors (Benson *et al.*, 1998; Walters *et al.*, 2000), however, β-CCB was still effective as an enhancer in both mutants, indicating that its effect was not due to interaction with the proposed sites; thus, the β-CCB binding site acting as enhancer on α3β2γ1 remains unknown. The $GABA_AR$ in OLs presented similar behavior with respect to the DZP high-affinity binding site, since the β-CCB positive modulatory effect was not antagonized by FMZ. This adds evidence supporting the idea that α3β2γ1 and the endogenous receptor are similar.

The modulatory effect on the endogenous receptor by β-CCB was due to a 5-fold increase in GABA sensitivity. Distinct β-carbolines presented differential potency on the oligodendroglial receptor, drugs that generated a net potentiating effect on the GABA response in OLs, such as β-CCB or β-CCE, did not have a prominent effect in neurons; thus, they can potentially be used as drugs to differentially stimulate GABAergic signaling in OLs. Lipophilicity of the β-carboline seems to be determinant for the interaction with the receptor, a highly lipophilic drug such as β-CCB had the greatest positive effect, while the most hydrophilic DMCM turns to be inhibitory in both cell types. This suggests that the enhancer binding site has relation with the receptor lipophilic microenvironment, thus probably the specific composition of the oligodendroglial and neuronal membranes would influence on the degree of inhibition or enhancement observed for the different drugs, a distinct lipidic microenvironment might also explain some differences observed using the heterologous expression model.

To give greater certainty about the participation of both α3 and γ1 subunits, these were specifically silenced in OPCs. Subunit silencing strongly decreased the corresponding protein expression and substantially changed the OPC GABA response. α3 subunit

Molecular Pharmacology Fast Forward. Published on December 7, 2020 as DOI: 10.1124/molpharm.120.000091
This article has not been copyedited and formatted. The final version may differ from this version.

silencing altered GABA sensitivity of the expressed receptor, as well as the receptor desensitization kinetics and the sensitivity to β-CCB. However, its peak amplitude remained unchanged, suggesting that the α3 absence was compensated by some other subunit conforming a different receptor; α1 and α2 subunits are candidates for this because both are expressed in OPCs, which would explain the increase in GABA sensitivity and the desensitization rate. In contrast, γ1 silencing caused a clear decrease in amplitude response, suggesting that γ1 is essential for the $GABA_AR$ expression in the OPC membrane; thus, this subunit is a plausible target to be downregulated in experiments designed for the study of GABAergic signaling function during the myelination process.

Together, these results provide pharmacological (use of β-carbolines) and genetic information that can be used to generate changes in the effectiveness of the $GABA_AR$ expressed in OLs and their precursor cells in the neonatal stage, which could be crucial to modify the status of GABAergic signaling in the context of its interaction with neurons during the first peak of myelination. The transcriptomic analyzes suggest that the proposed subunits remain well represented in OPCs until the adulthood, it is therefore likely that these subunits will be involved throughout life. Given that other subunits are co-expressed and that clearly there are differences of expression in different areas, participation of some other subunits cannot yet be completely ruled out.

Thus, evidence indicates that the endogenous $GABA_AR$ expressed in oligodendroglial lineage cells, from its OPC stage to premyelinating OLs, most likely contains the α3, β2, and γ1 subunits, this contributes to the determination of the oligodendroglial receptor structure that will allow molecular studies to characterize its function in the myelination process.

Molecular Pharmacology Fast Forward. Published on December 7, 2020 as DOI: 10.1124/molpharm.120.000091
This article has not been copyedited and formatted. The final version may differ from this version.

Molecular Pharmacology Fast Forward. Published on December 7, 2020 as DOI: 10.1124/molpharm.120.000091
This article has not been copyedited and formatted. The final version may differ from this version.

ACKNOWLEDGMENTS

We thank Jessica González Norris for editing this manuscript. We also thank Mr. Felipe Cornejo Ortiz, Dra. Nuri Aranda López, Lic. Ma. de Lourdes Lara Ayala, Ing. Elsa Nydia Hernández Ríos, M.V.Z. Martín García Servín, Dra. Alejandra Castilla León, Dr. Francisco J. Valles Valenzuela and Ing. Ramón Martínez Olvera for their expert technical support. A.C.-M. is a researcher from Cátedras-CONACYT commissioned at Instituto de Neurobiología in the Universidad Nacional Autónoma de México (UNAM). R.P.O., is a doctoral student from Programa de Doctorado en Ciencias Biomédicas of the Universidad Nacional Autónoma de México (UNAM) and received fellowship No. 700811 from CONACYT, México.

Molecular Pharmacology Fast Forward. Published on December 7, 2020 as DOI: 10.1124/molpharm.120.000091
This article has not been copyedited and formatted. The final version may differ from this version.

AUTHOR CONTRIBUTIONS

Participated in research design: Ordaz, Garay, Limon, Matute, and Arellano.

Conducted experiments: Ordaz, Garay, Pérez-Samartín, Sánchez-Gómez, Robles-Martínez, Cisneros-Mejorado, Matute, and Arellano.

Performed data analysis: Ordaz, Garay, Limon, Pérez-Samartín, Sánchez-Gómez, Cisneros-Mejorado, Matute, and Arellano.

Wrote the manuscript: The first draft of the manuscript was written by Ordaz and Arellano. All authors read, contributed, and approved the final manuscript.

Molecular Pharmacology Fast Forward. Published on December 7, 2020 as DOI: 10.1124/molpharm.120.000091
This article has not been copyedited and formatted. The final version may differ from this version.

REFERENCES

Arellano RO, and Miledi R (1993) Novel Cl^- currents elicited by follicle stimulating hormone and acetylcholine in follicle-enclosed *Xenopus* oocytes. *J Gen Physiol* **102**:833–857.

Arellano RO, Sánchez-Gómez MV, Alberdi E, Canedo-Antelo M, Chara JC, Palomino A, Pérez-Samartín A, and Matute C (2016) Axon-to-glia interaction regulates $GABA_A$ receptor expression in oligodendrocytes. *Mol Pharmacol* **89**:63–74.

Attali B, Wang N, Kolot A, Sobko A, Cherepanov V, and Soliven B (1997) Characterization of delayed rectifier Kv channels in oligodendrocytes and progenitor cells. *J Neurosci* **17**:8234–8245.

Baer K, Essrich C, Benson JA, Benke D, Bluethmann H, Fritschy J-M, Lü scher B, Hoffmann-La Roche F, and Roberts E (1999) Postsynaptic clustering of-aminobutyric acid type A receptors by the γ3 subunit *in vivo*. *PNAS* **96**:12860–12865.

Balia M, Benamer N, and Angulo MC (2017) A specific GABAergic synapse onto oligodendrocyte precursors does not regulate cortical oligodendrogenesis. *Glia* doi: 10.1002/glia.23197.

Balia M, Vélez-Fort M, Passlick S, Schäfer C, Audinat E, Steinhäuser C, Seifert G, and Angulo MC (2015) Postnatal down-regulation of the $GABA_A$ receptor γ2 subunit in neocortical NG2 cells accompanies synaptic-to-extrasynaptic switch in the GABAergic transmission mode. *Cereb Cortex* **25**:1114–1123.

Baraban M, Koudelka S, and Lyons DA (2018) Ca^{2+} activity signatures of myelin sheath formation and growth *in vivo*. *Nat Neurosci* **21**:19–23.

Molecular Pharmacology Fast Forward. Published on December 7, 2020 as DOI: 10.1124/molpharm.120.000091
This article has not been copyedited and formatted. The final version may differ from this version.

Belelli D, Lambert JJ, Peters JA, Wafford K, and Whiting PJ (1997) The interaction of the general anesthetic etomidate with the γ-aminobutyric acid type A receptor is influenced by a single amino acid. *Proc Natl Acad Sci USA* **94**:11031–11036.

Benson JA, Löw K, Keist R, Mohler H, and Rudolph U (1998) Pharmacology of recombinant γ-aminobutyric acid A receptors rendered diazepam-insensitive by point-mutated α-subunits. *FEBS Lett* **431**:400–404.

Bronstein JM, Hales TG, Tyndale RF, and Charles AC (1998) A conditionally immortalized glial cell line that expresses mature myelin proteins and functional $GABA_A$ receptors. *J Neurochem* **70**:483–491.

Cahoy JD, Emery B, Kaushal A, Foo LC, Zamanian JL, Christopherson KS, Xing Y, Lubischer JL, Krieg PA, Krupenko SA, Thompson WJ, and Barres BA (2008) A transcriptome database for astrocytes, neurons, and oligodendrocytes: a new resource for understanding brain development and function. *J Neurosci* **28**:264–278.

Cesetti T, Ciccolini F, and Li Y (2012) GABA not only a neurotransmitter: osmotic regulation by $GABA_AR$ signaling. *Front Cell Neurosci* **6**:1–14.

Cheli VT, Santiago González DA, Lama TN, Spreuer V, Handley V, Murphy GG, and Paez PM (2016) Conditional deletion of the L-type calcium channel $Ca_V1.2$ in oligodendrocyte progenitor cells affects postnatal myelination in mice. *J Neurosci* **36**:10853–10869.

Cheli VT, Santiago González DA, Spreuer V, and Paez PM (2015) Voltage-gated Ca^{2+} entry promotes oligodendrocyte progenitor cell maturation and myelination *in vitro*. *Exp Neurol* **265**:69–83.

Cisneros-Mejorado AJ, Garay E, Ortiz-Retana J, Concha L, Moctezuma JP, Romero S,

Molecular Pharmacology Fast Forward. Published on December 7, 2020 as DOI: 10.1124/molpharm.120.000091
This article has not been copyedited and formatted. The final version may differ from this version.

and Arellano RO (2019) Demyelination–remyelination of the rat caudal cerebellar peduncle evaluated with magnetic resonance imaging. *Neuroscience* doi: 10.1016/j.neuroscience.2019.06.042.

Dixon CL, Sah P, Keramidas A, Lynch JW, and Durisic N (2017) γ1-Containing $GABA_A$ receptors cluster at synapses where they mediate slower synaptic currents than γ2-containing $GABA_A$ receptors. *Front Mol Neurosci* **10**:1–16.

Dumont JN (1972) Oogenesis in *Xenopus laevis* (Daudin). I. Stages of oocyte development in laboratory maintained animals. *J Morphol* **136**:153–179.

Esmaeili A, Lynch JW, and Sah P (2009) $GABA_A$ receptors containing gamma1 subunits contribute to inhibitory transmission in the central amygdala. *J Neurophysiol* **101**:341–349.

Gilbert P, and Kettenmann H (1984) y-Aminobutyric acid directly depolarizes cultured oligodendrocytes. *J Neurosci* **4**:561–569.

Hamilton NB, Clarke LE, Arancibia-Carcamo IL, Kougioumtzidou E, Matthey M, Káradóttir R, Whiteley L, Bergersen LH, Richardson WD, and Attwell D (2017) Endogenous GABA controls oligodendrocyte lineage cell number, myelination, and CNS internode length. *Glia* **65**:309–321.

Hoppe D, and Kettenmann H (1989) GABA triggers a Cl^- efflux from cultured mouse oligodendrocytes. *Neurosci Lett* **97**:334–339.

Hosie AM, Dunne EL, Harvey RJ, and Smart TG (2003) Zinc-mediated inhibition of $GABA_A$ receptors: discrete binding sites underlie subtype specificity. *Nat Neurosci* **6**:362–369.

Jabs R, Pivneva T, Hüttmann K, Wyczynski A, Nolte C, Kettenmann H, and Steinhäuser C (2005) Synaptic transmission onto hippocampal glial cells with hGFAP promoter

activity. *J Cell Sci* **118**:3791–3803.

Kalakh S, and Mouihate A (2019) Enhanced remyelination during late pregnancy: involvement of the GABAergic system. *Sci Rep* **9**:1–16.

Kalanjati VP, Wixey JA, Miller SM, Colditz PB, and Bjorkman ST (2017) $GABA_A$ receptor expression and white matter disruption in intrauterine growth restricted piglets. *Int J Dev Neurosci* **59**:1–9.

Káradóttir R, Hamilton NB, Bakiri Y, and Attwell D (2008) Spiking and non-spiking classes of oligodendrocyte precursor glia in CNS white matter. *Nat Neurosci* **11**:450–456.

Karim N, Wellendorph P, Absalom N, Johnston GAR, Hanrahan JR, and Chebib M (2013) Potency of GABA at human recombinant $GABA_A$ receptors expressed in *Xenopus* oocytes: A mini review. *Amino Acids* **44**:1139–1149.

Kirchhoff F, and Kettenmann H (1992) GABA triggers a $[Ca^{2+}]_i$ increase in murine precursor cells of the oligodendrocyte lineage. *Eur J Neurosci* **4**:1049–1058.

Knoflach F, Rhyner T, Villa M, Kellenberger S, Drescher U, Malherbe P, Sigel E, and Möhler H (1991) The γ3-subunit of the $GABA_A$-receptor confers sensitivity to benzodiazepine receptor ligands. *FEBS Lett* **293**:191–194.

Krasnow AM, Ford MC, Valdivia LE, Wilson SW, and Attwell D (2018) Regulation of developing myelin sheath elongation by oligodendrocyte calcium transients *in vivo*. *Nat Neurosci* **21**:24–30.

Kukley M, Kiladze M, Tognatta R, Hans M, Swandulla D, Schramm J, and Dietrich D (2007) Glial cells are born with synapses. *FASEB J* **22**:2957–2969.

Larm JA, Cheung NS, and Beart PM (1996) (S)-5-fluorowillardiine-mediated neurotoxicity in cultured murine cortical neurones occurs via AMPA and kainate

receptors. *Eur J Pharmacol* **314**:249–254.

Larson VA, Zhang Y, and Bergles DE (2016) Electrophysiological properties of $NG2^+$ cells: Matching physiological studies with gene expression profiles. *Brain Res* **1638**:138–160.

Lin SC, and Bergles DE (2004) Synaptic signaling between GABAergic interneurons and oligodendrocyte precursor cells in the hippocampus. *Nat Neurosci* **7**:24–32.

Malherbe P, Sigel E, Baur R, Persohn E, Richards JG, and Möhler H (1990) Functional expression and sites of gene transcription of a novel α subunit of the $GABA_A$ receptor in rat brain. *FEBS Lett* **260**:261–265.

Marques S, Zeisel A, Codeluppi S, van Bruggen D, Mendanha Falcao A, Xiao L, Li H, Haring M, Hochgerner H, Romanov RA, Gyllborg D, Munoz-Manchado AB, La Manno G, Lonnerberg P, Floriddia EM, Rezayee F, Ernfors P, Arenas E, Hjerling-Leffler J, Harkany T, Richardson WD, Linnarsson S, and Castelo-Branco G (2016) Oligodendrocyte heterogeneity in the mouse juvenile and adult central nervous system. *Science* **352**:1326–1329.

Middendorp SJ, Maldifassi MC, Baur R, and Sigel E (2015) Positive modulation of synaptic and extrasynaptic $GABA_A$ receptors by an antagonist of the high affinity benzodiazepine binding site. *Neuropharmacology* **95**:459–467.

Orduz D, Maldonado PP, Balia M, Elez-Fort M, De Sars V, Yanagawa Y, Emiliani V, and Angulo MC (2015) Interneurons and oligodendrocyte progenitors form a structured synaptic network in the developing neocortex. *Elife* **4**:1–20.

Passlick S, Grauer M, Schafer C, Jabs R, Seifert G, and Steinhauser C (2013) Expression of the 2-subunit distinguishes synaptic and extrasynaptic $GABA_A$ receptors in NG2 cells of the hippocampus. *J Neurosci* **33**:12030–12040.

Pérez-Samartín A, Garay E, Moctezuma JPH, Cisneros-Mejorado A, Sánchez-Gómez MV, Martel-Gallegos G, Robles-Martínez L, Canedo-Antelo M, Matute C, and Arellano RO (2017) Inwardly rectifying K^+ currents in cultured oligodendrocytes from rat optic nerve are insensitive to pH. *Neurochem Res* **42**:2443–2455.

Pitman KA, and Young KM (2016) Activity-dependent calcium signalling in oligodendrocyte generation. *Int J Biochem Cell Biol* **77**:30–34.

Sánchez-Gómez MV, Serrano-Regal MP, Aberdi E, Pérez-Cerdá F, and Matute C (2018) Isolation, expansion, and maturation of oligodendrocyte lineage cells obtained from rat neonatal brain and optic nerve. *Methods Mol Biol* **1791**:95–113.

Sequeira A, Shen K, Gottlieb A, and Limon A (2019) Human brain transcriptome analysis finds region- and subject-specific expression signatures of $GABA_AR$ subunits. *Commun Biol* **2**:1–14.

Serrano-Regal MP, Luengas-Escuza I, Bayón-Cordero L, Ibarra-Aizpurua N, Alberdi E, Pérez-Samartín A, Matute C, and Sánchez-Gómez MV (2019) Oligodendrocyte differentiation and myelination is potentiated via $GABA_B$ receptor activation. *Neuroscience* doi: 10.1016/j.neuroscience.2019.07.014.

Serrano-Regal MP, Bayón-Cordero L, Ordaz RP, Garay E, Limon A, Arellano RO, Matute C, and Sánchez-Gómez MV (2020) Expression and Function of GABA Receptors in Myelinating Cells. *Front Cell Neurosci* **14**:1–15.

Shaw JC, Berry MJ, Dyson RM, Crombie GK, Hirst JJ, and Palliser HK (2019) Reduced neurosteroid exposure following preterm birth and its' contribution to neurological impairment: A novel avenue for preventative therapies. *Front Physiol* **10**:1–17.

Shaw JC, Palliser HK, Dyson RM, Berry MJ, and Hirst JJ (2018) Disruptions to the cerebellar GABAergic system in juvenile guinea pigs following preterm birth. *Int J*

Dev Neurosci **65**:1–10.

Sieghart W (2015) Allosteric modulation of $GABA_A$ receptors via multiple drug-binding sites, in *Advances in Pharmacology* (Rudolph U ed) pp 53–96, Elsevier Inc.

Tanaka Y, Tozuka Y, Takata T, Shimazu N, Matsumura N, Ohta A, and Hisatsune T (2009) Excitatory GABAergic activation of cortical dividing glial cells. *Oxford Univ Press* **19**:2181–2195.

Tasic B, Menon V, Nguyen TN, Kim TK, Jarsky T, Yao Z, Levi B, Gray LT, Sorensen SA, Dolbeare T, Bertagnolli D, Goldy J, Shapovalova N, Parry S, Lee C, Smith K, Bernard A, Madisen L, Sunkin SM, Hawrylycz M, Koch C, and Zeng H (2016) Adult mouse cortical cell taxonomy revealed by single cell transcriptomics. *Nat Neurosci* **19**:335–346.

Trudell JR, Yue ME, Bertaccini EJ, Jenkins A, and Harrison NL (2008) Molecular modeling and mutagenesis reveals a tetradentate binding site for Zn^{2+} in $GABA_A$ αβ receptors and provides a structural basis for the modulating effect of the γ subunit. *J Chem Inf Model* **48**:344–349.

Vélez-Fort M, Audinat E, and Angulo MC (2012) Central role of GABA in neuron-glia interactions. *Neuroscientist* **18**:237–250.

Vélez-Fort M, Maldonado PP, Butt AM, Audinat E, and Angulo MC (2010) Postnatal switch from synaptic to extrasynaptic transmission between interneurons and NG2 cells. *J Neurosci* **30**:6921–6929.

von Blankenfeld G, Trotter J, and Kettenmann H (1991) Expression and developmental regulation of a $GABA_A$ receptor in cultured murine cells of the oligodendrocyte lineage. *Eur J Neurosci* **3**:310–316.

Wafford KA, Bain CJ, Whiting PJ, and Kemp JA (1993) Functional comparison of the

role of γ subunits in recombinant human γ-aminobutyric acid A/benzodiazepine receptors. *Mol Pharmacol* **44**:437–442.

Wake H, Ortiz FC, Woo DH, Lee PR, Angulo MC, and Fields RD (2015) Nonsynaptic junctions on myelinating glia promote preferential myelination of electrically active axons. *Nat Commun* doi: 10.1038/ncomms8844.

Walters RJ, Hadley SH, Morris KD, and Amin J (2000) Benzodiazepines act on $GABA_A$ receptors via two distinct and separable mechanisms. *Nat Neurosci* **3**:1274–1281.

Williamson A V., Mellor JR, Grant AL, and Randall AD (1998) Properties of $GABA_A$ receptors in cultured rat oligodendrocyte progenitor cells. *Neuropharmacology* **37**:859–873.

Wingrove PB, Wafford KA, Bain C, and Whiting PJ (1994) The modulatory action of loreclezole at the gamma-aminobutyric acid type A receptor is determined by a single amino acid in the β2 and β3 subunit. *Proc Natl Acad Sci U S A* **91**:4569–73.

Ymer S, Draguhn1 A, Wisden W, Werner P, Keinanen K, Schofield3 PR, Sprengel R, Pritchett DB, Seeburg PH, Feld IN, and Zellphysiologie A (1990) Structural and functional characterization of the γ1 subunit of $GABA_A$/benzodiazepine receptors. *EMBO J* **9**:3261–3267.

Ymer S, Schofield' PR, Draguhn2 A, Werner P, Kohier M, and Seeburg3 PH (1989) $GABA_A$ receptor β subunit heterogeneity: functional expression of cloned cDNAs. *EMBO J* **8**:1665–1670.

Zhang Y, Chen K, Sloan SA, Bennett ML, Scholze AR, Phatnani HP, Paolo Guarnieri X, Caneda C, Ruderisch N, Deng S, Liddelow SA, Zhang C, Daneman R, Maniatis T, Ben Barres XA, and Jia Qian Wu X (2014) An RNA-sequencing transcriptome and splicing database of glia, neurons, and vascular cells of the cerebral cortex. *J*

Neurosci **34**:11929–11947.

Zonouzi M, Scafidi J, Li P, McEllin B, Edwards J, Dupree JL, Harvey L, Sun D, Hübner CA, Cull-Candy SG, Farrant M, and Gallo V (2015) GABAergic regulation of cerebellar NG2 cell development is altered in perinatal white matter injury. *Nat Neurosci* **18**:674–682.

Molecular Pharmacology Fast Forward. Published on December 7, 2020 as DOI: 10.1124/molpharm.120.000091
This article has not been copyedited and formatted. The final version may differ from this version.

FOOTNOTE

This study was supported by grants from CONACYT-México No. 252121 and PAPIIT UNAM-México No. IN203519 to R.O.A. laboratory; NIH [R21AG053740 and R21MH113177] and the Amon G. Carter Foundation to A.L., and by grants from CIBERNED (CB06/05/0076) and the Ministry of Economy and Competitiveness, Government of Spain (SAF2016-75292-R) and Basque Government (IT1203-19) to C.M..

Some information reported herein was presented during a poster session by Rainald Pablo Ordaz, Edith Garay, Carlos Matute, and Rogelio O. Arellano at the “XIV European Meeting on Glial Cells in Health and Disease, GLIA 2019” on July 10-13, 2019.

Molecular Pharmacology Fast Forward. Published on December 7, 2020 as DOI: 10.1124/molpharm.120.000091
This article has not been copyedited and formatted. The final version may differ from this version.

FIGURE LEGENDS

Fig. 1. Diversity of $GABA_AR$ subunit expression in murine OPCs and OLs. A) mRNA expression level for the 19 known $GABA_AR$ subunit genes analyzed in PDGFRα$^+$ cells isolated by fluorescence-activated cell sorting from mice brains and assessed by RNA-Seq. The expression level of each $GABA_AR$ subunit is represented as its fractional contribution (FC) to the total pool of RNA available to produce $GABA_AR$ subunits. Data were obtained from http://www.brainrnaseq.org. B) $GABA_AR$ subunit RNA expression analysis from PDGFRα$^+$ cells from cortex (S1 and V1) and corpus callosum of adult mice. The expression level is represented as its FC to all RNA $GABA_AR$ subunits available like in A). Data were obtained from Gene Expression Omnibus (GSE75330) and https://celltypes.brain-map.org/rnaseq. C) The gel shows amplification by RT-PCR of $GABA_AR$ subunit sequences expressed in purified OLs from rat P12 optic nerve. The expected product lengths are 266, 1311, 354, 231, 404 and corresponded to α3, β2, β3, γ1 and γ3 subunits, respectively (bp, base pairs; MW, molecular weight marker; C(-), reaction negative control). D) Analysis by immunocytochemistry of forebrain OPCs maintained in culture. Panels show images of the fluorescence signal for a specific antibody against the $GABA_AR$ subunit proteins (in green) as indicated in each panel, and nuclei labeling with DAPI (blue). Bars = 50 μm.

Fig. 2. Heterologous functional expression of oligodendroglial $GABA_AR$ subunits cloned from rat optic nerve. A) The cRNA for $GABA_AR$ α3, β2, β3, γ1 and γ3 subunits was synthesized and injected in different combinations into *Xenopus* oocytes as indicated. The expressed GABA responses were monitored electrophysiologically for

Molecular Pharmacology Fast Forward. Published on December 7, 2020 as DOI: 10.1124/molpharm.120.000091
This article has not been copyedited and formatted. The final version may differ from this version.

each combination. In this and subsequent records, GABA was applied during the times indicated by bars at the top, and oocytes were held at -60 mV. D-R curves were constructed and plotted as illustrated; each point represents the average peak response (mean ± S.D.) normalized with respect to maximal current response elicited by 1 mM GABA monitored in 10-25 oocytes from 3-5 frogs. B) Comparison of the peak current (mean ± S.D.) by 1 mM GABA generated in each of the combinations studied. Each bar includes 9-19 oocytes from five donors. α3β2γ1 mean amplitude response was different to all others. C) The graph built from data in A) shows a comparison of the combinations containing αβγ subunits signaling the decrease in GABA sensitivity due to the presence of the γ1 subunit. The EC_{50} differences were statistically significant between the receptors containing γ1 versus those containing γ3. *$p < 0.001$ for comparisons across the mean of -logEC_{50} values from each subunit combination, one-way ANOVA followed by a Tukey's *post hoc* Test.

Fig. 3. Effect of Zn^{2+} on $GABA_A$Rs expressed in *Xenopus* oocytes from oligodendroglial sequences. A) The traces illustrate the responses to 100 μM GABA in the absence (gray trace in each case) and presence of 100 μM Zn^{2+} (black trace) for each receptor studied as indicated. B) The percentage of GABA response achieved in the presence of Zn^{2+} in each condition was normalized against the response generated without Zn^{2+}, then averaged and plotted in the bar graph (mean ± S.D.; 7-10 oocytes from 3-5 frogs). γ3 subunit conferred resistance to inhibition by Zn^{2+} similar to γ2 subunit, while presence of γ1 allowed inhibition of the GABA-response close to 50% and was statistically different to those receptors without γ subunit or containing either γ2 or

Molecular Pharmacology Fast Forward. Published on December 7, 2020 as DOI: 10.1124/molpharm.120.000091
This article has not been copyedited and formatted. The final version may differ from this version.

γ3. One-way ANOVA ($p < 0.001$) followed by a *post hoc* Tukey test showed that all values were statistically different from each other.

Fig. 4. Dose-response (D-R) to Zn^{2+} of $GABA_A$Rs expressed in *Xenopus* oocytes from oligodendroglial sequences. A) Top traces illustrate responses evoked by 10 μM GABA in the presence of different Zn^{2+} concentrations as indicated in each case for the α3β2, α3β2γ1 and α3β3γ1 receptors expressed heterologously. B) The response amplitude from recordings obtained in A) were normalized with respect to the control GABA response, without Zn^{2+}, in the same oocytes, and the inhibition D-R curves were plotted to obtain the IC_{50} in each receptor. Data points represent the average (± S.D.) of 5-7 oocytes (from 3 frogs) in each condition. Comparisons were made between the mean of the -logIC_{50} values of each combination of subunits. The one-way ANOVA ($p < 0.001$) followed by a *post hoc* Tukey test showed that all values were statistically different from each other.

Fig. 5. Pharmacological effect of allosteric modulators on the GABA response of α3β2γ1 receptors expressed in oocytes. A) Traces illustrate the modulatory effect of drugs (10 μM; DZP, β-CCB or indiplon) co-applied with GABA (10 μM) in each case; control response with GABA alone is shown in black. The mean effect response observed in 11 oocytes (5-6 frogs) was plotted in B) including the effect of Zn^{2+} in the same group of oocytes for comparison. C) Traces illustrate the effect of 10 μM FMZ, a specific antagonist for the high affinity BZP binding site. It shows the response to 10 μM GABA alone, followed by the effect of 30 μM β-CCB in the absence and presence of

Molecular Pharmacology Fast Forward. Published on December 7, 2020 as DOI: 10.1124/molpharm.120.000091
This article has not been copyedited and formatted. The final version may differ from this version.

FMZ that did not antagonize the enhancement caused by β-CCB. The mean effect response obtained in 7 oocytes is shown in the bar graph. The increase in GABA response by β-CCB plus FMZ was statistically significant against the group without FMZ (*$p < 0.001$, paired two-tailed Student's t-test). D) Effect of 3 μM β-CCB on the GABA response activated in α3β2 receptors without γ subunit, or those containing either γ1 or γ3. Mean responses (6-10 oocytes from 3 frogs) were statistically different for the 3 receptors compared with the control response elicited by GABA alone, and β-CCB enhancement in α3β2γ1 response was different to all others. *$p < 0.001$ one-way ANOVA followed by a Tukey's *post hoc* test.

Fig. 6. The α3β2γ1 receptor BZP binding sites and the enhancement caused by β-CCB. A) 1 μM DZP or 3 μM β-CCB were co-applied with 10 μM GABA to analyze its effect on the high affinity site for BZP. Traces illustrate the responses obtained in oocytes that were injected with the cRNA of the native α3β2γ1 subunits (left column), and in oocytes injected with the α3(H126R)β2γ1 mutant (right column). The average responses obtained in 5-6 oocytes are shown in the bar graph indicating that DZP enhancement was eliminated, whereas the β-CCB enhancement was maintained in the mutated combination (line at 100% indicates control response to GABA). B) Similar experiments in A) were performed applying 60 μM DZP or 3 μM β-CCB co-applied with 10 μM GABA to analyze its effect on one of the low-affinity BZP sites. In the left column, the traces illustrate the responses obtained in oocytes expressing the native α3β2γ1 subunits, while the second group expresses the mutant α3(S294I)β2(N264I)γ1(S282I). The averages of the responses obtained in 10 oocytes (3 frogs) are shown in the bar

Molecular Pharmacology Fast Forward. Published on December 7, 2020 as DOI: 10.1124/molpharm.120.000091
This article has not been copyedited and formatted. The final version may differ from this version.

graph indicating that DZP enhancement was strongly reduced while the increase generated by β-CCB was maintained in the mutated combination. All drug effects were statistically significant against the control group, with the clear exception of the mutant tested with DZP in A) ($p < 0.001$ for comparisons between the control vs. drug-treated amplitude values, unpaired two-tailed Student's t-Test).

Fig. 7. β-CCB modulatory effect on the GABA response elicited in the oligodendroglial lineage. A) GABA current response was monitored electrophysiologically in OLs (from optic nerve) or cortical neurons held at -80 mV. The enhancement mediated by either 10 μM DZP (orange bar) or 10 μM β-CCB (blue bar), in the presence and absence of 10 μM FMZ, was analyzed as summarized in the bar graph. The first black bar in each data set shows the control GABA response in the absence of drugs; the second bar of each group indicates the average of the response in the presence of a modulator; the gray bar indicates the modulator effect plus FMZ. The washing effect is in black. FMZ did not antagonize the response to β-CCB in OLs, but it was strongly effective on the potentiating DZP effect in both OLs and cortical neurons (10 μM GABA was used for OLs while 3 μM GABA for neurons). B) D-R curves for GABA in OLs in the absence (black) and presence of 10 μM β-CCB (blue). Each data point represents the average response to GABA in 8 OLs in both conditions. Data were adjusted to a D-R curve. Traces to the right illustrate the GABA current response in the presence of 10 μM β-CCB; in this and subsequent records in neural cells, drugs were applied as indicated by the top bars and cells were held at -80 mV.

Molecular Pharmacology Fast Forward. Published on December 7, 2020 as DOI: 10.1124/molpharm.120.000091
This article has not been copyedited and formatted. The final version may differ from this version.

Fig. 8. β-carbolines modulatory effect on GABA current responses from either OLs or cortical neurons. A) The response to 10 μM GABA in the absence and presence of a β-carboline (10 μM) was tested in OLs from the optic nerve. Each drug indicated from 1 to 6 corresponds to the structures in the lower part of the Figure, and traces illustrate the current response obtained for 3 drugs tested as indicated. Bars are the average of the normalized response with respect to the control response without β-carboline (100% line in graph) for each of the cells registered (6-21 cells in each case). The traces in gray correspond to control current responses, while black traces are the GABA responses in the presence of a β-carboline. B) For comparison, a similar analysis was performed for the GABA response elicited in cortical neurons (6-8 cells in each case) by applying 3 μM GABA and the same set of β-carbolines. Traces illustrate responses obtained for the 3 drugs indicated, in gray correspond to control current responses, while green traces are the GABA responses in the presence of a β-carboline. All drug effects were statistically significant against the control group with exception of β-CHM in OLs, as well as β-CCB and β-CCE in neurons ($p < 0.001$ for comparisons between the control cells versus β-carboline treated cells, unpaired two-tailed Student's t-Test).

Fig. 9. α3 $GABA_AR$ subunit silencing in cells of the oligodendroglial lineage. A) Images illustrate α3 subunit immunodetection (in green, nuclei in blue) in OPCs maintained in culture. The first panel depicts cells without treatment (untreated). The cells designated as α3-siRNA were transfected with specific interfering sequences

Molecular Pharmacology Fast Forward. Published on December 7, 2020 as DOI: 10.1124/molpharm.120.000091
This article has not been copyedited and formatted. The final version may differ from this version.

against the subunit, while control cells were processed for transfection with scramble sequences. All groups correspond to cells 72 h after the transfection process. The estimated α3 expression in AUF was normalized with respect to the untreated group as shown in the bar graph (average of 7 slices from 3 transfected cultures). B) Analysis of responses evoked by 1 mM GABA in control and α3-siRNA treated cells. Traces correspond to typical records in both conditions where the desensitization kinetics was adjusted to an exponential curve to estimate the time constant (τ) decay, and the graphs show the amplitude response and τ values for each group, where each data point represents the response of one cell. The mean ± S.D. is shown in gray in each case. C) Traces illustrate GABA D-R curves built for both groups; in the graph, each data point represents the mean ± S.D. of the normalized response in 10 cells. Lines are the best fit to D-R curves and broken lines indicate the corresponding EC_{50}. D) Traces illustrate typical response in control (black), and α3-siRNA treated cells (red) evoked by GABA (10 μM) alone, or co-applied with 10 μM of β-CCB (blue trace). Bar graph shows the amplitude (mean ± S.D., in gray) response values for each group, where each data point represents the response in a single cell. *$p < 0.001$ for comparisons between the control cells versus α3-siRNA treated cells, unpaired two-tailed Student's t-Test.

Fig. 10. γ1 $GABA_AR$ subunit silencing in cells of the oligodendroglial lineage. A) Images illustrate γ1 subunit immunodetection (in green, nuclei in blue) in OPCs maintained in culture. The first panel shows the untreated cells. The γ1-siRNA group represents cells transfected with specific interfering sequences against the subunit. Control cells were processed for transfection with scramble sequences. B) After 72 h,

Molecular Pharmacology Fast Forward. Published on December 7, 2020 as DOI: 10.1124/molpharm.120.000091
This article has not been copyedited and formatted. The final version may differ from this version.

the expression of γ1 was estimated in AUF and the values were normalized with respect to the untreated group (average of 7 slices from 3 transfected cultures). Also, traces illustrate responses elicited by 1 mM GABA in control and γ1-siRNA treated cells. The response amplitude for each group is represented in the graph. Each data point is the amplitude obtained in a single cell, and the mean ± S.D. is indicated in gray. C) Traces illustrate GABA D-R curves built for both groups, where each data point represents the mean ± S.D. of the normalized response in 17-20 cells, and lines are the best fit to D-R curves. D) Traces illustrate typical response in control (black), and γ1-siRNA treated cells (light blue) evoked by GABA (10 μM) alone, or co-applied with 10 μM of β-CCB (dark blue trace). Bar graph shows the amplitude (mean ± S.D., in gray) response values for each group, where each data point represents the response in a single cell. *p < 0.001 for comparisons between the control cells versus γ1-siRNA treated cells, unpaired two-tailed Student's t-Test.

A

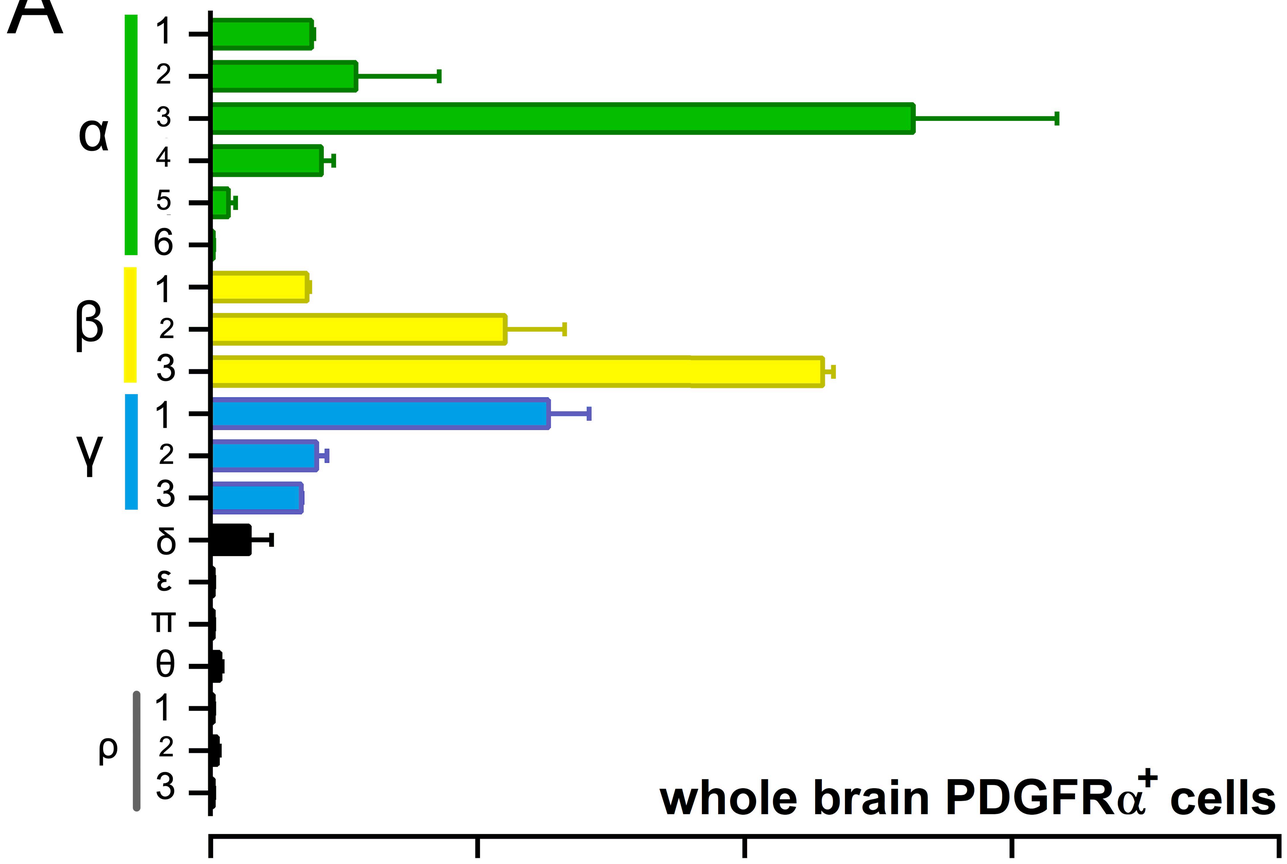

B

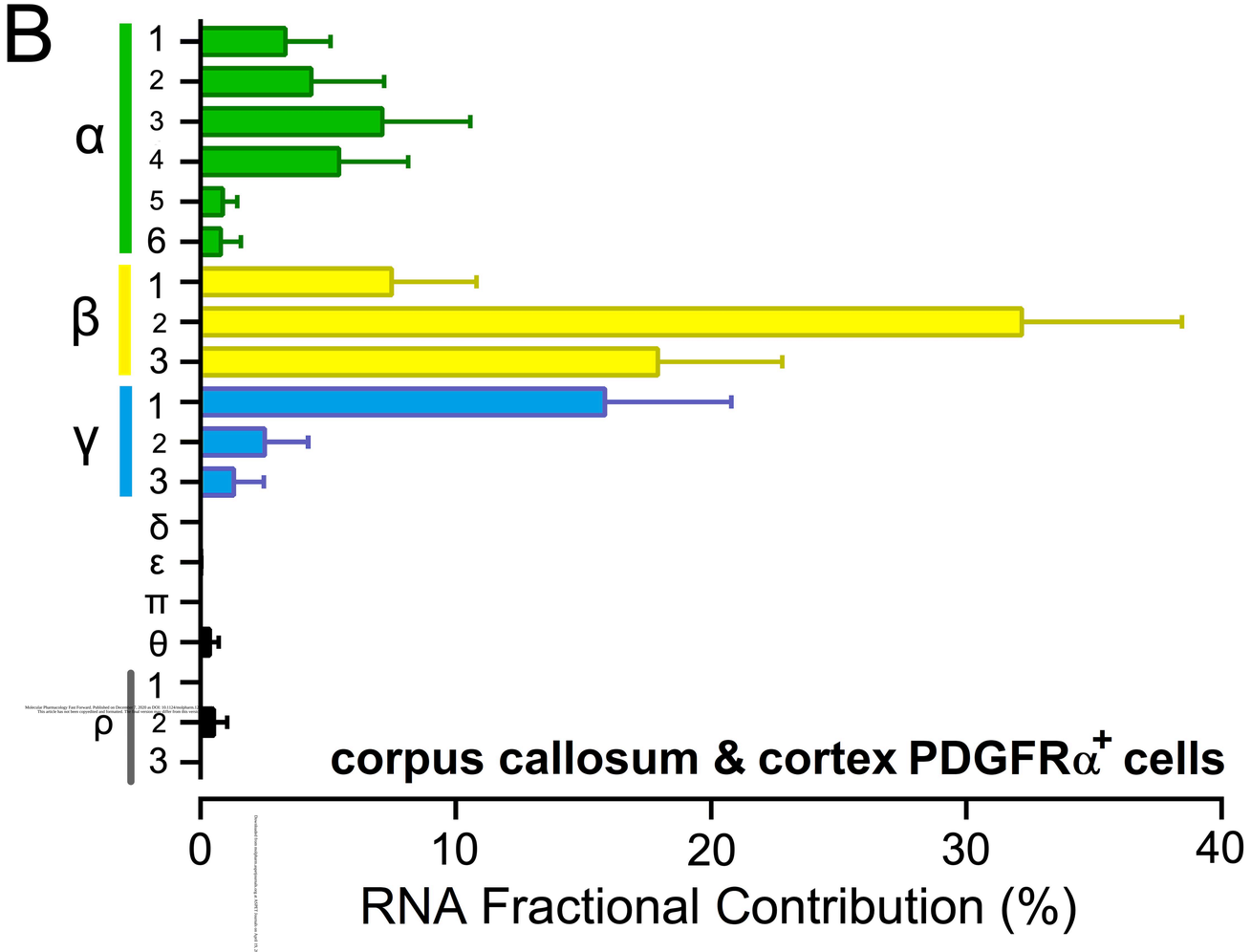

C

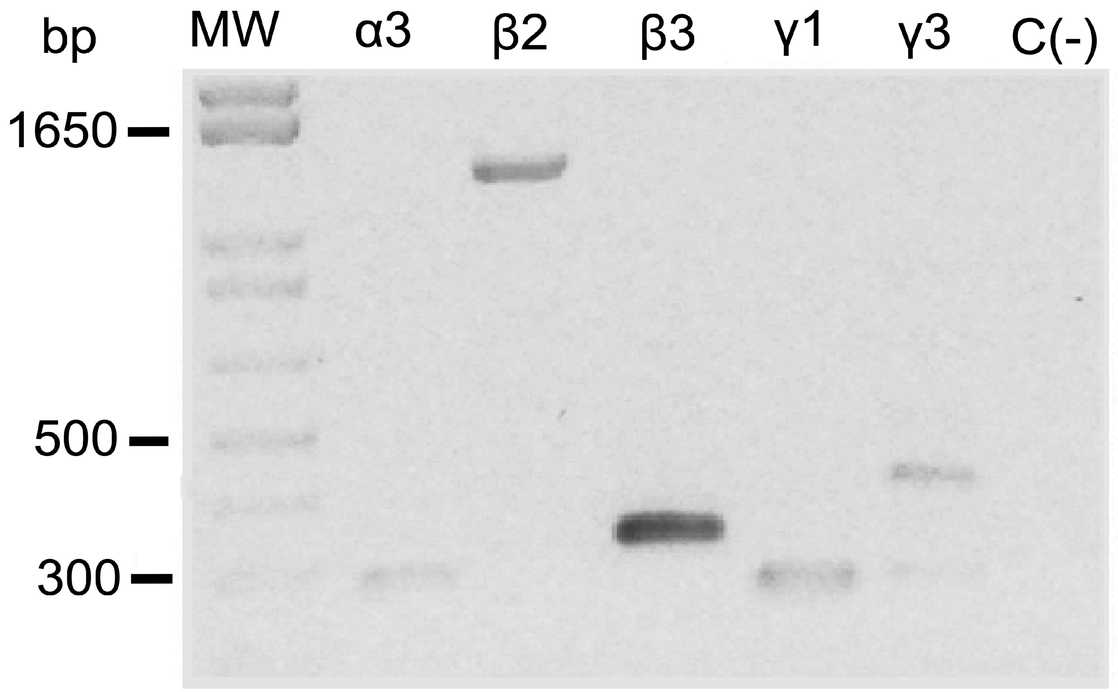

D

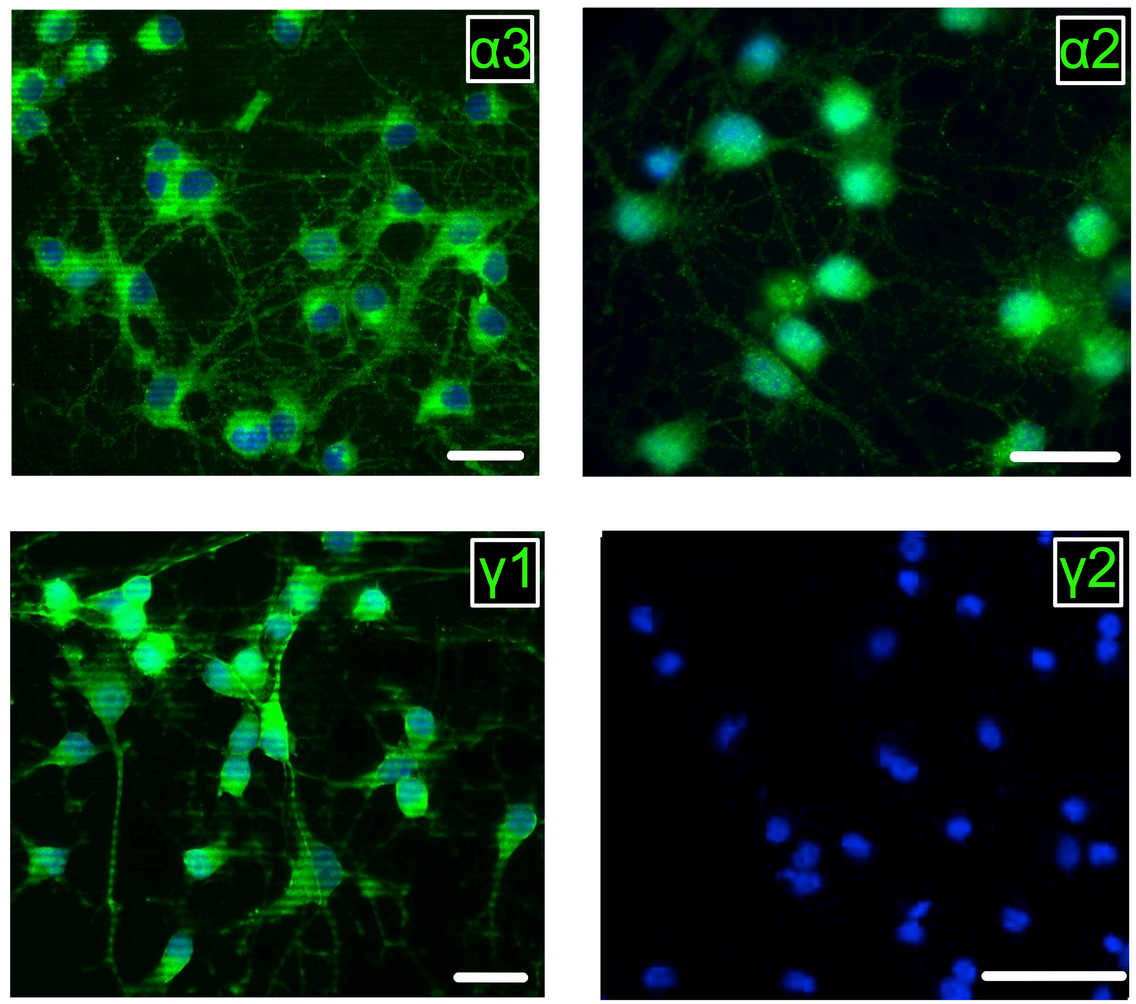

Figure 1

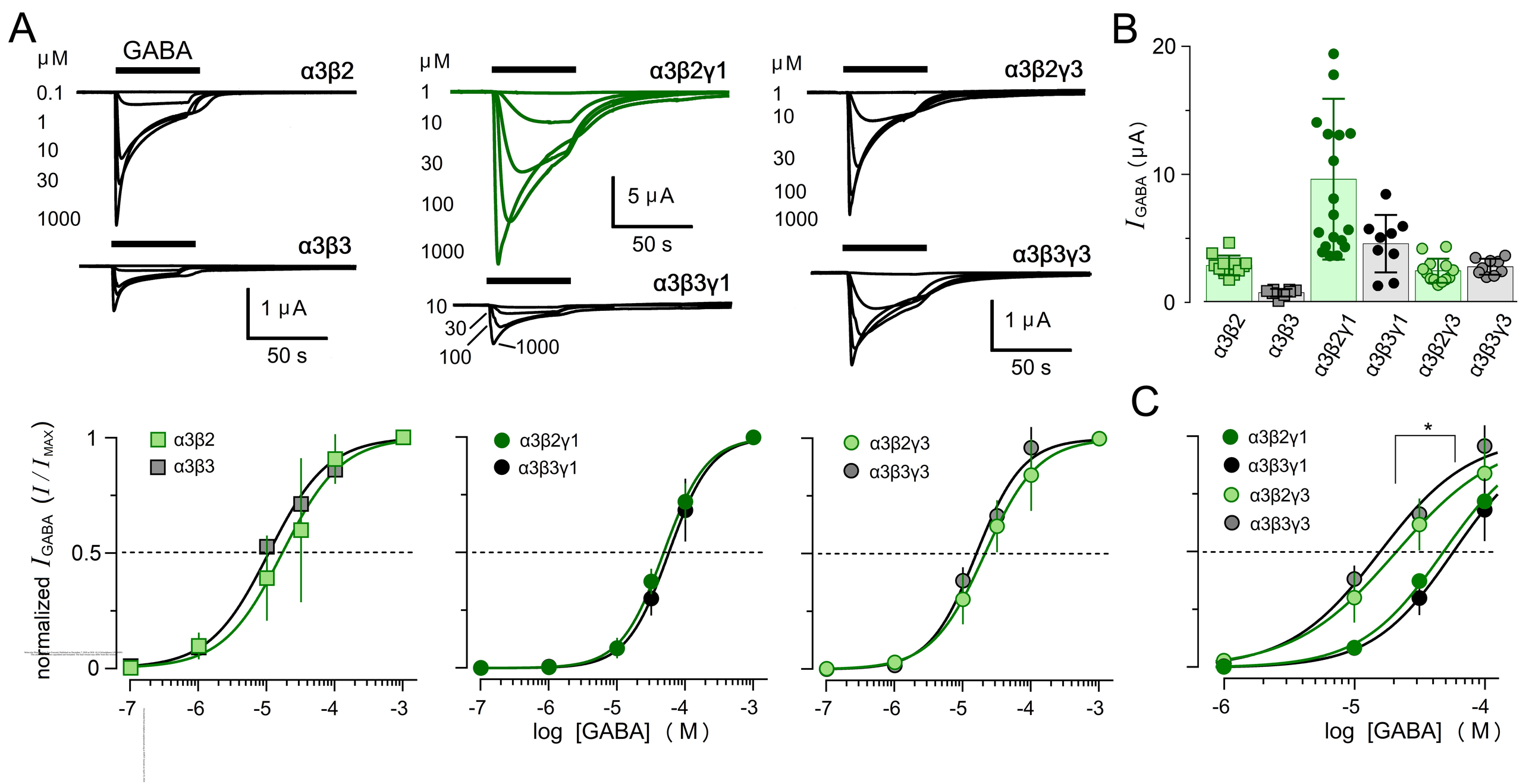
A
GABA
μM
0.1
1
10
30
1000
α3β2
α3β3
1 μA
50 s
μM
1
10
30
100
1000
α3β2γ1
5 μA
50 s
α3β3γ1
10
30
100
1000
μM
1
10
30
100
1000
α3β2γ3
α3β3γ3
1 μA
50 s
B
20
10
0
I_{GABA} (μA)
α3β2
α3β3
α3β2γ1
α3β3γ1
α3β2γ3
α3β3γ3
C
normalized I_{GABA} (I / I_{MAX})
1
0.5
0
α3β2
α3β3
α3β2γ1
α3β3γ1
α3β2γ3
α3β3γ3
*
-7
-6
-5
-4
-3
log [GABA] (M)

Figure 2

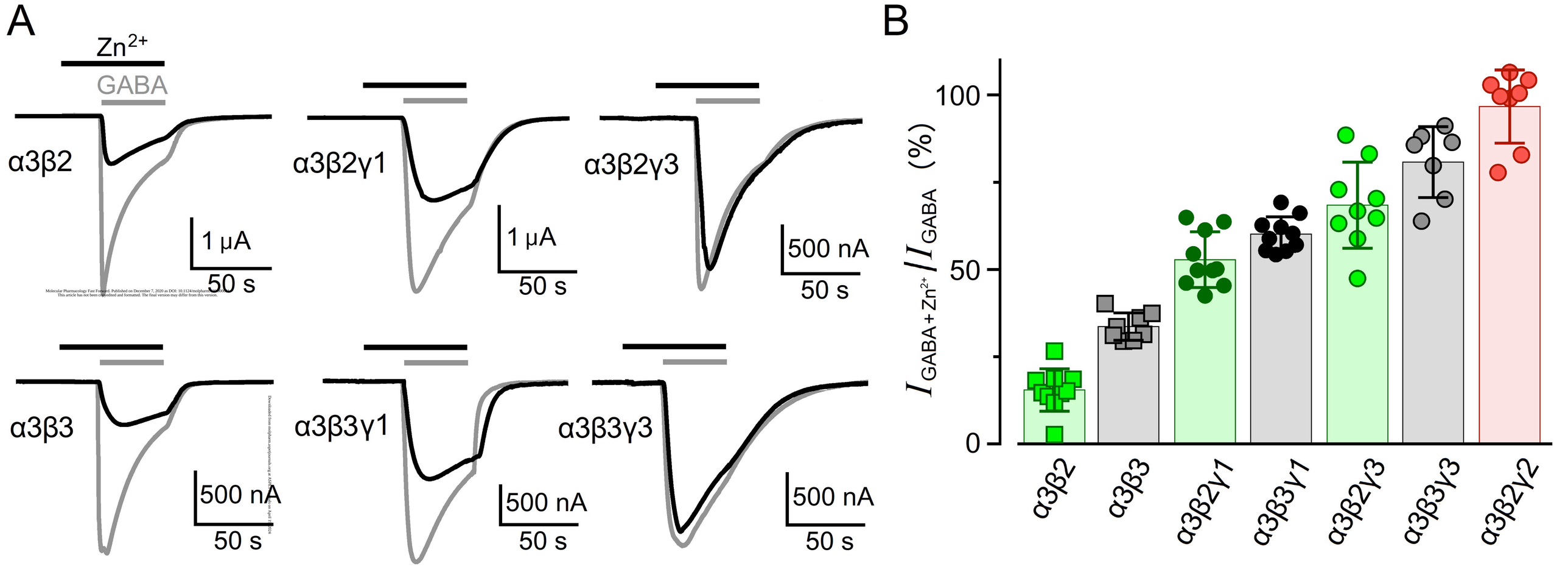

Figure 3

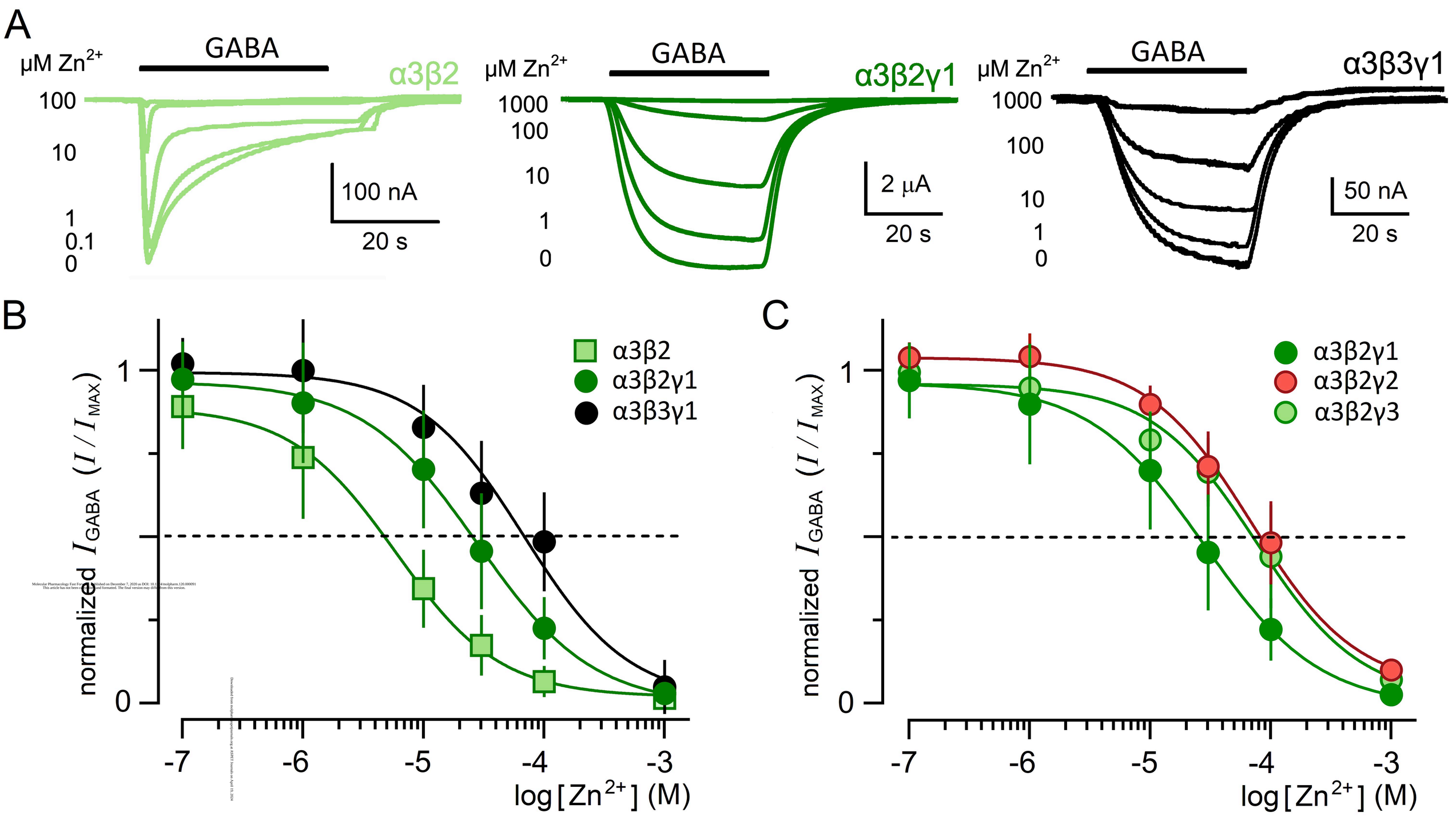

Figure 4

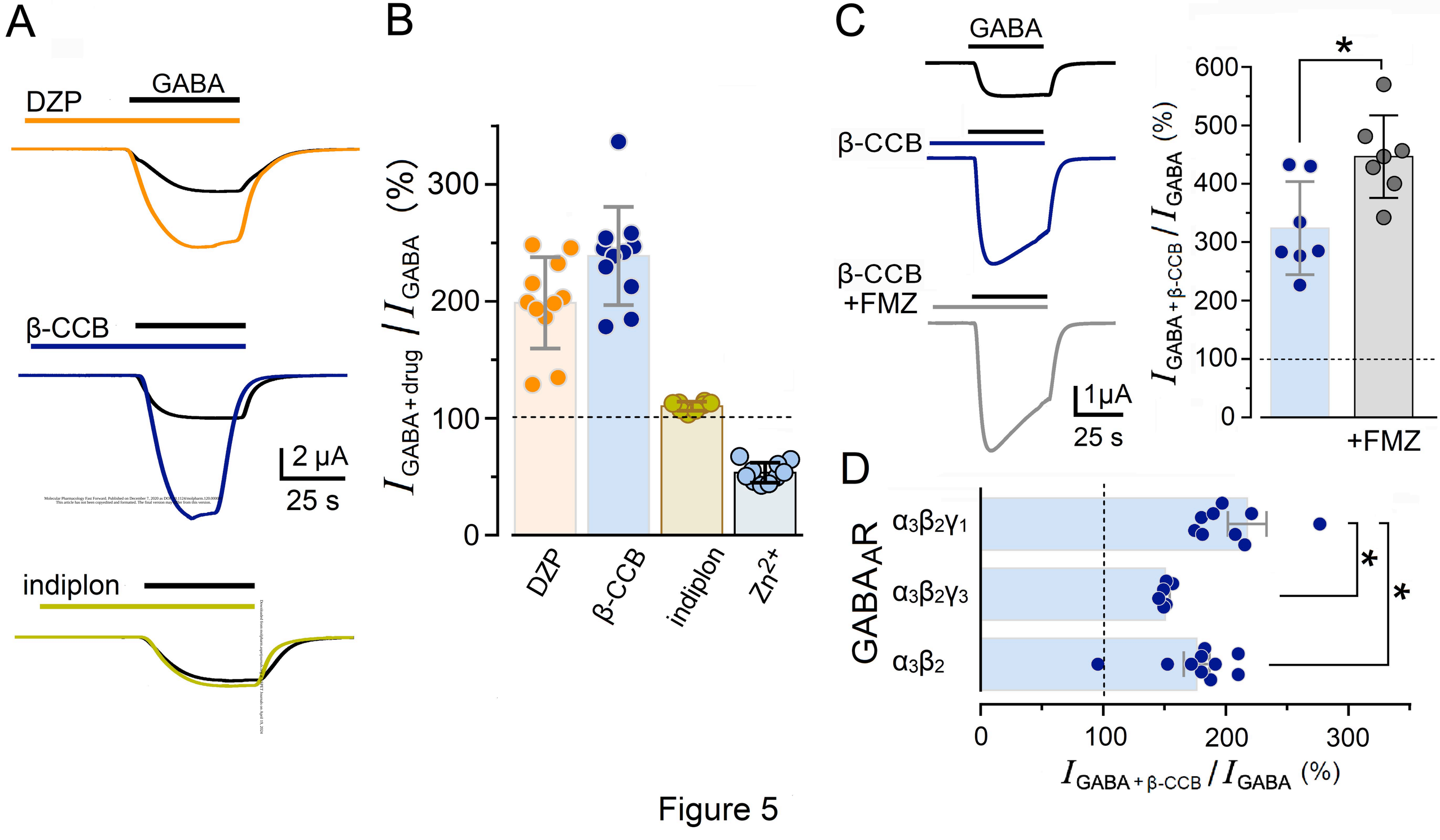

Figure 5

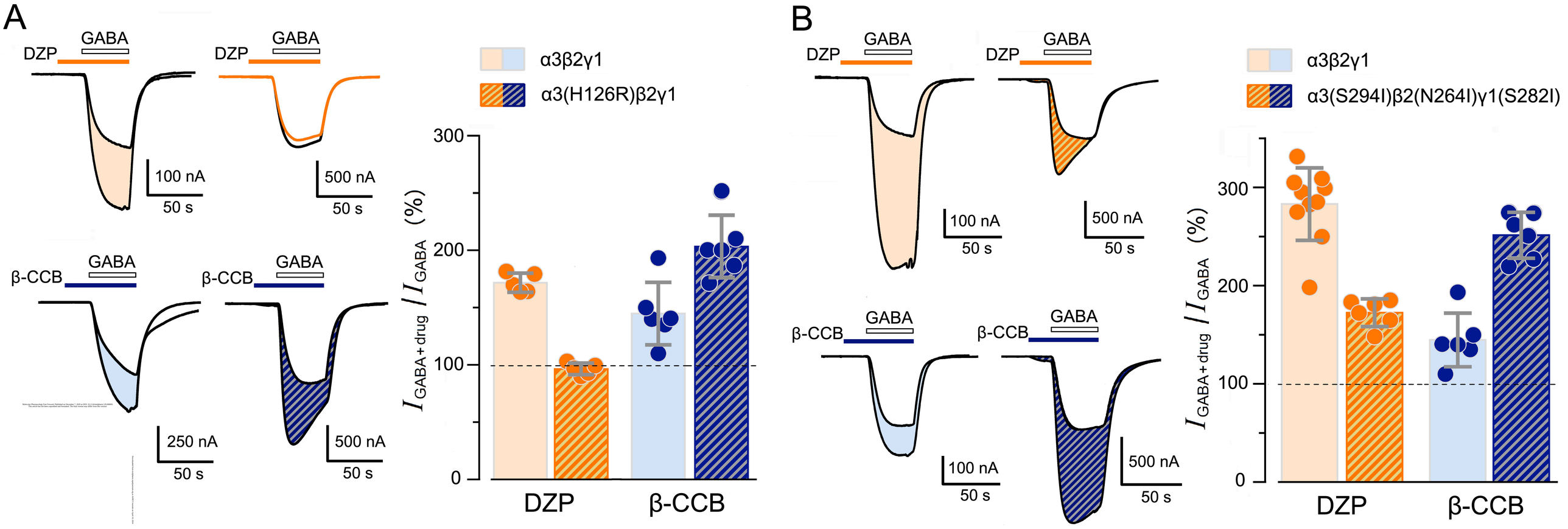
A
DZP
GABA
100 nA
50 s
DZP
GABA
500 nA
50 s
β-CCB
GABA
250 nA
50 s
β-CCB
GABA
500 nA
50 s
α3β2γ1
α3(H126R)β2γ1
300
200
100
0
$I_{GABA+drug} / I_{GABA}$ (%)
DZP
β-CCB
B
DZP
GABA
100 nA
50 s
DZP
GABA
500 nA
50 s
β-CCB
GABA
100 nA
50 s
β-CCB
GABA
500 nA
50 s
α3β2γ1
α3(S294I)β2(N264I)γ1(S282I)
300
200
100
0
$I_{GABA+drug} / I_{GABA}$ (%)
DZP
β-CCB

Figure 6

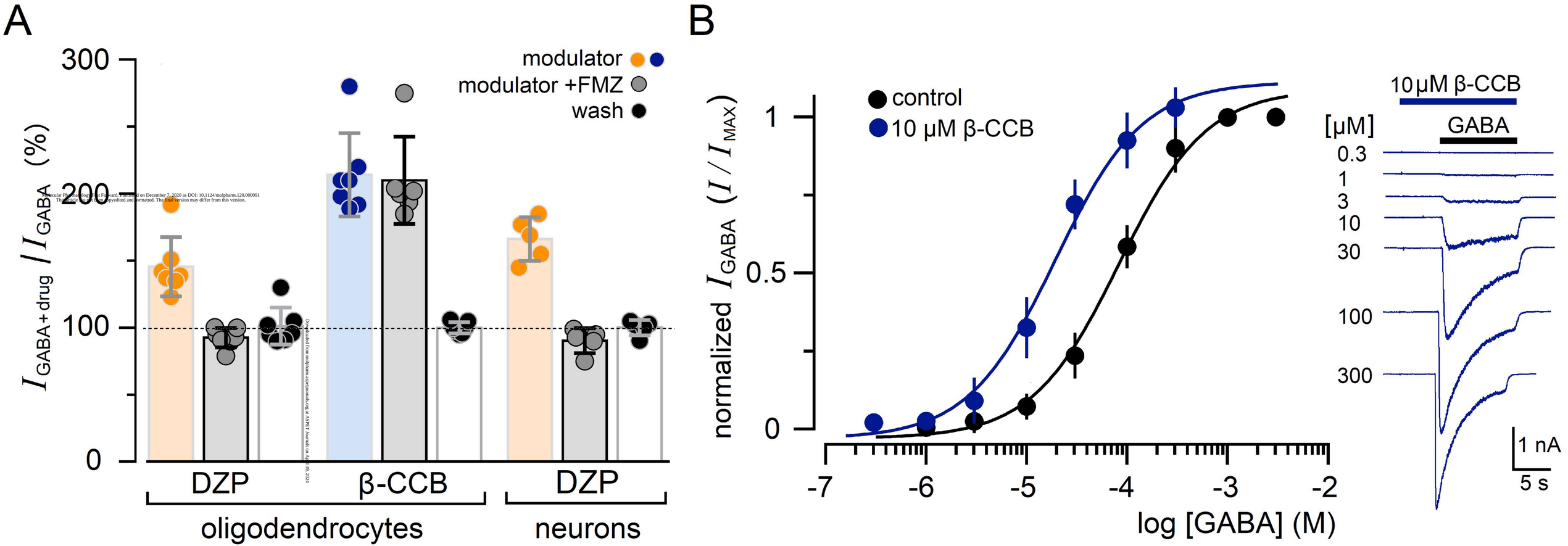

Figure 7

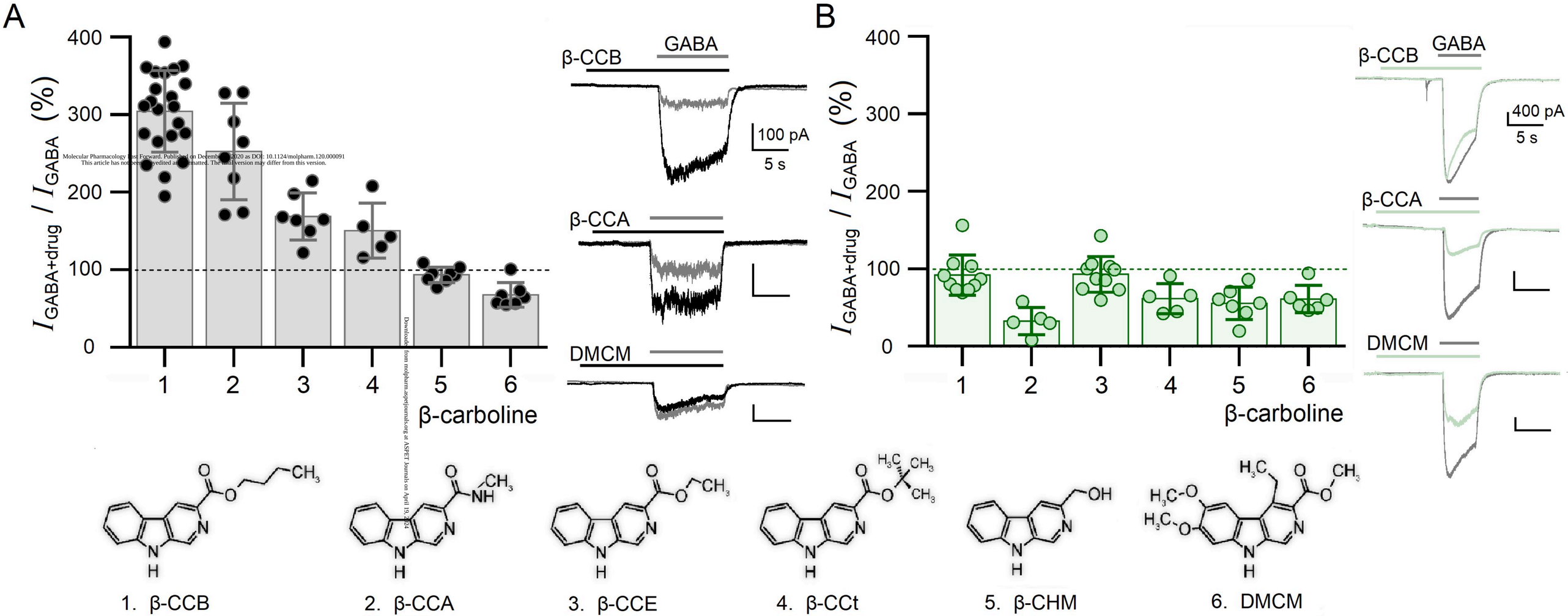

Figure 8

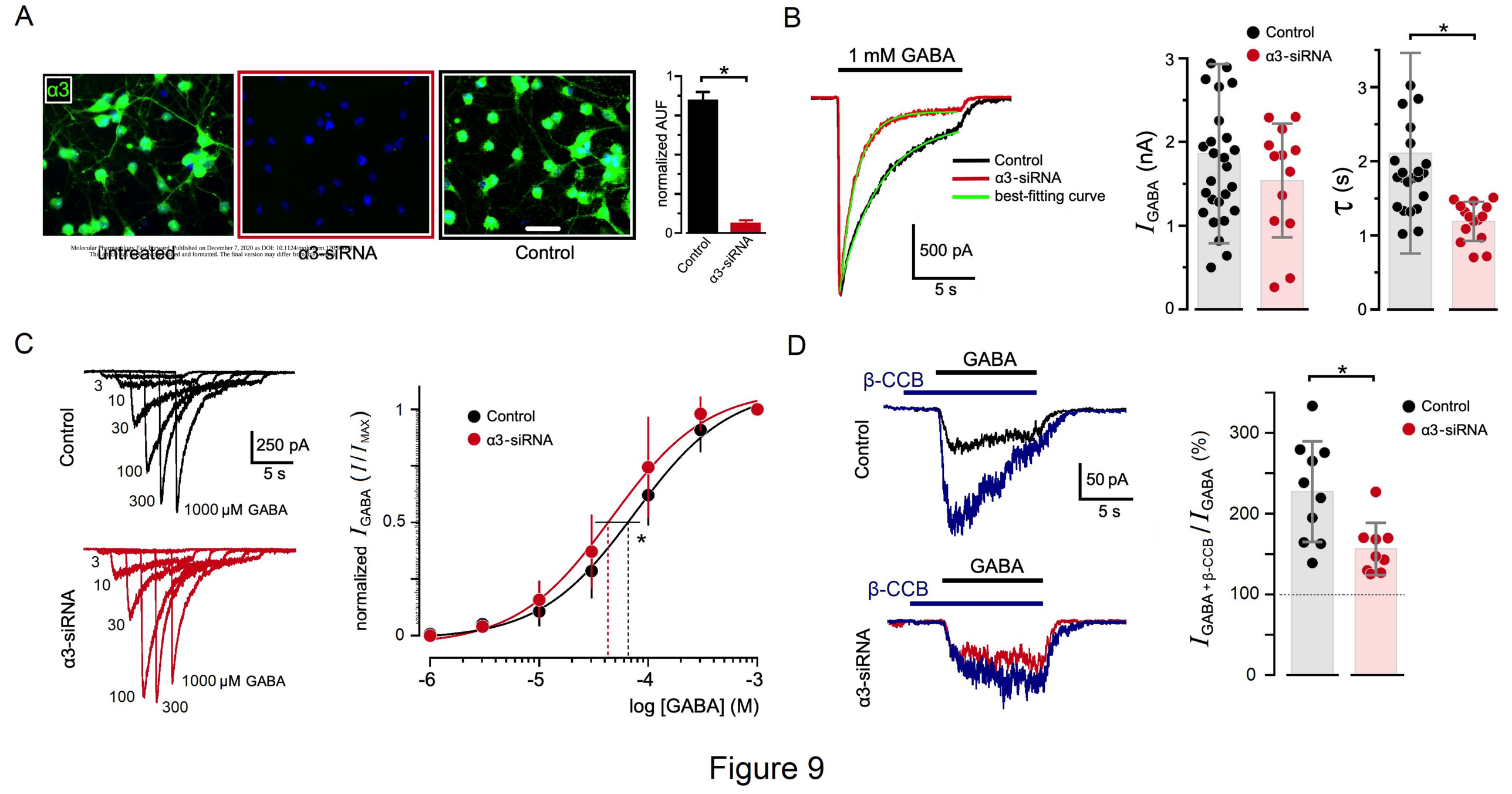

Figure 9

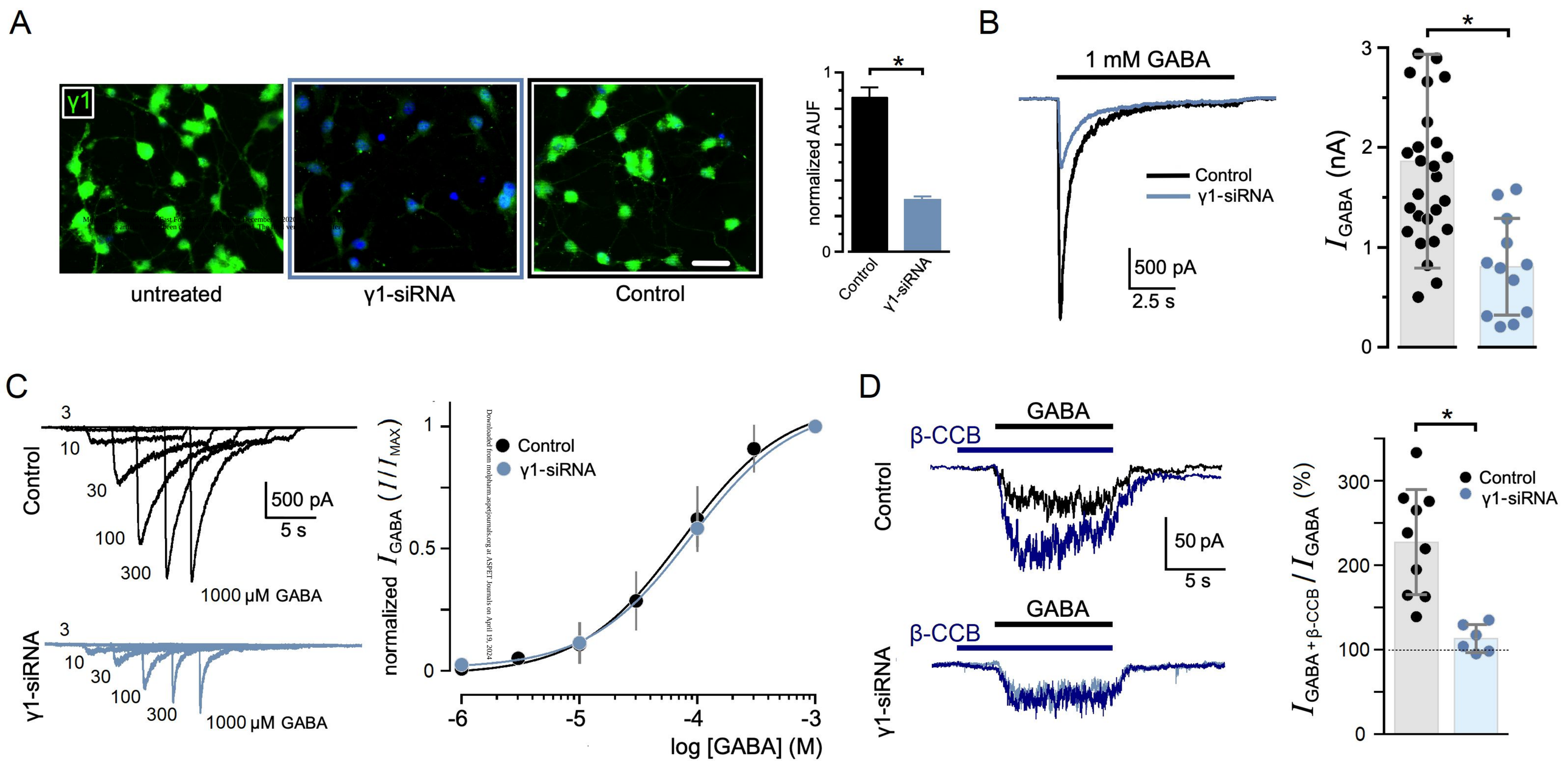
A
γ1
untreated
γ1-siRNA
Control
normalized AUF
Control
γ1-siRNA
B
1 mM GABA
Control
γ1-siRNA
500 pA
2.5 s
I_{GABA} (nA)
C
Control
γ1-siRNA
3
10
30
100
300
1000 μM GABA
500 pA
5 s
normalized I_{GABA} (I/I_{MAX})
log [GABA] (M)
D
GABA
β-CCB
50 pA
5 s
$I_{GABA+β-CCB}$ / I_{GABA} (%)

Figure 10